Hautier L, Billet G, de Thoisy B, Delsuc F. 2017. Beyond the carapace: skull shape variation and morphological systematics of long-nosed armadillos (genus *Dasypus*) PeerJ 5:e3650 https://doi.org/10.7717/peerj.3650

Beyond the carapace: skull shape variation and morphological systematics of long-nosed armadillos (genus *Dasypus*)

Lionel Hautier Corresp., [1, 2] , **Guillaume Billet** [3] , **Benoit De Thoisy** [4] , **Frédéric Delsuc** [1]

[1] Institut des Sciences de l'Evolution de Montpellier, Université de Montpellier, Montpellier, France
[2] Mammal Section, Life Sciences, Vertebrate Division, The Natural History Museum, London, United Kingdom
[3] Museum national d'Histoire naturelle, Paris, France
[4] Institut Pasteur de la Guyane, Cayenne, France

Corresponding Author: Lionel Hautier
Email address: lionel.hautier@umontpellier.fr

Background. The systematics of long-nosed armadillos (genus *Dasypus*) has been mainly based on a handful of external morphological characters and classical measurements. Here, we studied the pattern of morphological variation in the skull of long-nosed armadillos species, with a focus on the systematics of the widely distributed nine-banded armadillo (*D. novemcinctu*s). **Methods.** We present the first exhaustive 3D comparison of the skull morphology within the genus *Dasypus*, based on µCT-scans. We used geometric morphometric approaches to explore the patterns of the intra- and interspecific morphological variation of the skull with regard to several factors such as taxonomy, geography, allometry, and sexual dimorphism. **Results.** We show that the shape and size of the skull vary greatly between *Dasypus* species, with *D. pilosus* representing a clear outlier compared to other long-nosed armadillos. The study of the cranial intraspecific variation in *D. novemcinctus* evidences clear links to the geographic distribution and argue in favour of a revision of past taxonomic delimitations. Our detailed morphometric comparisons detected previously overlooked morphotypes of nine-banded armadillo, especially a very distinctive unit circumscribed to the Guiana Shield. **Discussion.** As our results are congruent with recent molecular data and analyses of the structure of paranasal sinuses, we propose that *D. novemcinctus* should be regarded either as a polytypic species (with three to four subspecies) or as a complex of several distinct species.

PeerJ Preprints | https://doi.org/10.7287/peerj.preprints.2924v1 | CC BY 4.0 Open Access | rec: 12 Apr 2017, publ: 12 Apr 2017

Beyond the carapace: skull shape variation and morphological systematics of long-nosed armadillos (genus *Dasypus*).

Lionel Hautier[1,2], Guillaume Billet[3], Benoit de Thoisy[4,5], and Frédéric Delsuc[1]

[1]Institut des Sciences de l'Evolution, UMR5554, CNRS, IRD, EPHE, Université de Montpellier, Montpellier, France.
[2]Mammal Section, Life Sciences, Vertebrate Division, The Natural History Museum, Cromwell Road, London SW7 5BD, UK.
[3]Sorbonne Universités, CR2P, UMR 7207, CNRS, Université Paris 6, Muséum National d'Histoire Naturelle, Paris, France.
[4]Institut Pasteur de la Guyane, Cayenne, French Guiana.
[5]Kwata NGO, BP 972, Cayenne, French Guiana.

Corresponding Author
Lionel Hautier
Email address: lionel.hautier@umontpellier.fr.

Abstract

Background. The systematics of long-nosed armadillos (genus *Dasypus*) has been mainly based on a handful of external morphological characters and classical measurements. Here, we studied the pattern of morphological variation in the skull of long-nosed armadillos species, with a focus on the systematics of the widely distributed nine-banded armadillo (*D. novemcinctu*s).

Methods. We present the first exhaustive 3D comparison of the skull morphology within the genus *Dasypus*, based on µCT-scans. We used geometric morphometric approaches to explore the patterns of the intra- and interspecific morphological variation of the skull with regard to several factors such as taxonomy, geography, allometry, and sexual dimorphism.

Results. We show that the shape and size of the skull vary greatly between *Dasypus* species, with *D. pilosus* representing a clear outlier compared to other long-nosed armadillos. The study of the cranial intraspecific variation in *D. novemcinctus* evidences clear links to the geographic distribution and argues in favour of a revision of past taxonomic delimitations. Our detailed morphometric comparisons detected previously overlooked morphotypes of nine-banded armadillos, especially a very distinctive unit circumscribed to the Guiana Shield.

Discussion. As our results are congruent with recent molecular data and analyses of the structure of paranasal sinuses, we propose that *D. novemcinctus* should be regarded either as a polytypic species (with three to four subspecies) or as a complex of several distinct species.

Introduction

With their Pan-American distribution, long-nosed armadillos (genus *Dasypus*) constitute an understudied model for Neotropical biogeography. They are the most taxonomically diverse and widespread extant xenarthrans. The genus *Dasypus* traditionally comprises seven extant species (*D. novemcinctus*, *D. hybridus*, *D. septemcinctus*, *D. kappleri*, *D. pilosus*, *D. mazzai*, and *D. sabanicola*; Wetzel, 1985; Wilson & Reeder, 2005; Feijo & Cordeiro-Estrela, 2014) and two extinct ones (*D. bellus* and *D. punctatus*; Castro et al., 2013; Castro, 2015). In spite of being one of the earliest diverging cingulate lineages (Gaudin & Wible, 2006; Delsuc et al., 2012; Gibb et al., 2016), the dasypodid early evolutionary history remains poorly known (Castro, 2015). Only three extinct genera were recognized among the Dasypodini: *Anadasypus* from the middle Miocene of Colombia and late Miocene of Ecuador (Carlini, Vizcaíno & Scillato-Yané, 1997; Carlini et al., 2013), *Pliodasypus* from the late Pliocene of Venezuela (Castro et al., 2014), and *Propraopus* from the middle Pleistocene–early Holocene of South America (Castro et al., 2013a).

Aside the widespread nine-banded armadillo (*D. novemcinctus*), all extant long-nosed armadillos are restricted to South America. Some species are sympatric in certain areas resulting in competition and possibly supporting divergent behaviours and morphologies. The nine-banded armadillo is likely to be the most abundant armadillo in tropical forests (Wetzel & Mondolfi, 1979; Loughry & Mcdonough, 1998) and has the widest distribution of all extant xenarthran species. Its distribution is thought to cover much of South and Central America and parts of North America and ranges from the south-east United States to North western Argentina and Uruguay (McBee & Baker, 1982). The species ability to disperse quickly, as well as its opportunistic and generalist mode of life, could partly explain this large distribution (Smith &

Doughty, 1984; Loughry & Mcdonough, 1998) marked by its rapid historical expansion into the United States (Taulman & Robbins, 2014). Such a wide geographical distribution, combined with early-recognized morphological variations (Peters, 1864; Gray, 1873; Allen, 1911; Lönnberg, 1913; Russell, 1953), raise the possibility that major taxonomic subgroups have been overlooked, be it at the subspecific or even specific level.

As its vernacular name implies, the genus *Dasypus* is characterized by a long, slender rostrum, which represents at least more than 55% of the length of the head (Gardner, 2008). The different species are usually distinguished by body and cranial measurements, colour differences, and morphological features of the carapace such as the number of movable bands and scutes across the body and the number and shape of osteodermal foramina (Feijo & Cordeiro-Estrela, 2016). The carapace is a hallmark of armadillos, and constitutes such a unique feature for mammals that it has dominated the attention of early and modern anatomists and, as a result, partly jeopardized the classification of the group. Its morphology, chiefly the number of movable bands, has been intensively, if not abusively, used in systematic studies. However, even in the so-called nine-banded armadillo, the number of movable bands can vary from 7 to 10 (Wetzel & Mondolfi, 1979). Yet early on, in his Systema Naturae (ed. 10, p. 51), (Linnaeus, 1758) casted doubt on the use of the number of movable bands as a criterion to distinguish *Dasypus* species (*i.e.*, *D. septemcinctus* from *D. novemcinctus*). Since then, a number of authors have raised the question whether such external features could be confidently used for systematic purposes. Wetzel and Mondolfi (1979) argued that "although many scientific names of armadillos are based on the number of movable bands, it is proposed here that for vernacular names we discontinue using this variable characteristic and base names upon unique or more consistent features". In the early 20th century, Hamlett (1939) made similar observations when focusing on the nine-banded armadillo; he considered as impossible to recognize external variations at a subspecific level and concluded that “cranial characters appear to offer the only promise for subspecific analysis of the species” (Hamlett 1939:335). We decided to take up and further discuss Hamlett’s idea since no large review of the dasypodine cranial variation has been undertaken to date.

This study aims to further elucidate the pattern of morphological variation seen in the skull of long-nosed armadillos, with a focus on the nine-banded armadillo. Geometric morphometric data were collected for most *Dasypus* species using µCT-scans. The main questions asked in the present study were whether different patterns of variation in skull shape can be characterized among and within long-nosed armadillo species, and if those patterns could be linked to factors such as taxonomy, geographical distribution, skull size, or sexual dimorphism. Our ultimate goals are to reconstruct the details of the biogeographic distribution of the widespread nine-banded armadillo at the continental scale and to lay the path for a new integrative taxonomy of long-nosed armadillos. A greater understanding of the morphological diversity and patterns of evolution for long-nosed armadillos is timely to effectively conserve these species and will also serve to deepen our knowledge of their peculiar evolution and biology (Loughry & Mcdonough, 2013).

Materials & Methods

Biological samples

The material studied came from the collections of the *Muséum national d’Histoire naturelle* in Paris (MNHN, collections *Zoologie et Anatomie comparée, Mammifères et Oiseaux*), the Natural History Museum in London (BMNH), the Naturalis Biodiversity Center in Leiden (NBC), the

Royal Ontario Museum in Toronto (ROM), the Louisiana State University in Bâton-Rouge (LSU), the American Museum of Natural History in New York (AMNH), the National Museum of Natural History in Washington (USNM), the *Instituto de Pesquisas Científicas e Tecnológicas do Estado do Amapá* in Macapá (IEPA), and the *Muséum d'Histoire naturelle* in Geneva, the KWATA association in Cayenne, and the Personal collection of Pierre Charles-Dominique. We analysed 128 skulls belonging to five *Dasypus* species (see Table S1 for a complete list of specimens): *D. novemcinctus*, *D. hybridus*, *D. septemcinctus*, *D. kappleri*, and *D. pilosus* (no data was available for *D. yepesi*, and *D. sabanicola*). With these data we performed a preliminary assessment of the average amounts of cranial variation at the specific level among different populations of *D. novemcinctus* from French Guiana, Guyana, Suriname, Ecuador, Brazil, Venezuela, Colombia, Costa Rica, Belize, Bolivia, Argentina, Paraguay, Uruguay, Panama, Nicaragua, Honduras, Guatemala, Mexico, Peru, and USA (Table S1). Juvenile, subadult, and adult specimens were considered in order to take into account the effect of age, size and differential growth on the dataset. Several studies (Hensel, 1872; Russell, 1953; Ciancio, Castro & Asher, 2012) showed that long-nosed armadillos possess tooth replacement, as typical for mammals, and that the eruption of permanent teeth occurs relatively late, as observed in afrotherians (Asher & Lehmann, 2008). Accordingly, we used eruption of the teeth, suture closure, and size as criteria to identify adult specimens in our dataset.

Geometric morphometric methods

Due to the limitations of the classical qualitative descriptive approach, geometric morphometrics represents a good complementary technique by which to examine intraspecific shape variation. Digital data of all specimens were acquired using X-ray micro-computed tomography (µCT) at the University of Montpellier (France), at the Natural History Museum (London, UK), and at the AST-RX platform MNHN (Paris, France). Three-dimensional reconstruction and visualization of the skulls were performed using stacks of digital μCT images with AVIZO v. 6.1.1 software (Visualization Sciences Group 2009). The mandibles and crania of armadillos were quantified with 10 and 84 anatomical landmarks respectively (Fig. 1 and Tables 1 and 2) using ISE-MeshTools (version 1.3.1; Lebrun, 2014). These landmarks were inspired by previous studies performed on different mammalian taxa (Hautier, Lebrun & Cox, 2012; Hautier et al., 2014). Considering the tendency to the reduction of the number of teeth in *Dasypus* specimens (Allen, 1911), which often lack the last dental locus and thus produce an artificial shortening of the entire tooth row, we decided to place a landmark after the seventh teeth and not at the end of the tooth row as it is usually the norm. Since skulls were often incomplete, the number of landmarks was adjusted to account for the maximal morphological variation in a maximum number of individuals; this number was then different whether we performed analyses considering all *Dasypus* species (10 and 84 landmarks for the mandible and the cranium respectively) or only *D. novemcinctus* (10 and 82 landmarks for the mandible and the cranium respectively).

All configurations (sets of landmarks) were superimposed using the Procrustes method of generalized leastsquares superimposition (GLS scaled, translated, and rotated configurations so that the intralandmark distances were minimized) following the methods of Rohlf (1999) and Bookstein (1991). Subsequently, mandibular and cranial forms of each specimen were represented by centroid size S, and by multidimensional shape vector v in linearized Procrustes shape space. Shape variability of the skull and the mandible was analysed by Principal Component Analysis (PCA) of shape (Dryden & Mardia, 1998). Analysis and visualization of patterns of shape variation were performed with the interactive software package

MORPHOTOOLS (Specht, 2007; Specht, Lebrun & Zollikofer, 2007; Lebrun, 2008; Lebrun et al., 2010).

To account for the potentially confounding effects of size allometry on shape, size-corrected shapes were obtained as follows. In a first step, allometric patterns were obtained via regression of Procrustes coordinates against the logarithm of centroid size, yielding an allometric shape vector (ASV), which characterizes cranial allometric patterns. In a second step, regressions of Procrustes coordinates against the logarithm of centroid size were computed for all species, yielding species-specific allometric shape vectors (ASVs). The ASVs represent directions in shape space that characterize species-specific allometric patterns of shape variation. A common allometric shape vector (ASVc), obtained as the mean of all the ASVs, provided a direction in shape space that minimizes potential divergence in mandibular allometric patterns across species (see Lebrun et al., 2010 for further details concerning this methodology). PCres corresponds to principal components of a PCA performed on shape data corrected for allometry. The same analyses have been performed at the intraspecific level and regressions were then computed between the Procrustes coordinates and the logarithm of centroid size for all subgroups (defined at a country level).

Multivariate analyses of variance (MANOVA) were performed on the principal component scores of mandibular and cranial mean shapes (35 first PCs, i.e. 90% of the variance) in order to assess the effects of different factors on mandibular and cranial shape variation: clades (species), sex, and geographic distribution (countries). MANOVAs were performed with Past 2.06 (Hammer, Harper & Ryan, 2001). Linear discriminant analyses (LDA) of shape coordinates were performed on the same number of PCs to assess a potential discrimination of skull morphology in relation to phylogeny (*i.e.*, species) and geography (*i.e.*, countries). When a group included only one individual, this specimen was integrated into the dataset as ungrouped cases. A skull from Panama (USNM 171052) was not complete enough to be considered in these analyses. We then decided to perform similar analyses with a reduced set of landmarks (71 landmarks on the cranium) to enable morphological comparisons with other specimens.

Linear measurements

Several linear measurements of the skull of *Dasypus* were calculated directly on 3D coordinates of landmarks (Fig. 2). These measurements were used to compare our results with traditional methods of species delineation.

Results

Interspecific variation of skull shape among long-nosed armadillos

A MANOVA performed on the first 35 PCs (i.e. 90% of the variance) indicates a significant morphological differentiation of the mandibles and crania relative to species delimitations (mandible Wilks' lambda=0.01164, F=4.903, p<0.001; cranium Wilks' lambda=0.0005897, F=11, p<0.001). A multivariate regression of the shape component on size, estimated by the logarithm of centroid size, was highly significant for the skull (mandible Wilks' lambda=0.2709, F=6.637, p<0.001; cranium Wilks' lambda=0.0632, F=30.92, p<0.001). When looking at the allometric shape vectors obtained with the centroid size, we found that size explains 18.99% and 25.58% of the variation in the whole mandibular and cranial data sets respectively (S2A and S3A).

Morphological differences occur among the mandibles of the five species of *Dasypus* (Fig. 3A). The first two principal components (24.73 % and 16.48% of total shape variation) weakly discriminates *D. pilosus* (negative values) from *D. kappleri* (positive values) while all specimens of *D. novemcinctus*, *D. hybridus*, and *D. septemcinctus* sit in the middle of the graph. These axes separate mandibles having a slender horizontal ramus with an elongated anterior part (located in front of the tooth row) and a short ascending ramus with a short coronoid process anteriorly positioned and vertically oriented from mandibles showing a high horizontal ramus with a short anterior part and a long ascending ramus with an elongated and distally oriented coronoid process. Mandibles of different size are poorly discriminated along the first principal component (Fig. 3B). Once the effect of allometry is removed (S4), no clear morphological differentiation is visible along PCres1. All taxa but *D. pilosus* lay in the positive values of PCres2 therefore the variation in this component is mostly restricted to this latter species.

The interspecific differences in the cranium of *Dasypus* are apparent in the morphospace defined by the first two principal components. Except for *D. hybridus* and *D. septemcinctus*, all species are well discriminated in the morphospace defined by the two first principal components (Fig. 4A), which explain 28,4% and 14,6% of the variance respectively. The first principal component unequivocally discriminates *D. hybridus* and *D. septemcinctus* from other species, and negatively correlates with a shortened rostrum and enlarged basicranium and braincase (Fig. 4A). *D. pilosus* individuals are well discriminated on the second principal component. On PC2 (Fig. 4A), the crania of *D. pilosus* appear narrower with a long snout and smaller braincase (positive values) whereas the crania of *D. novemcinctus*, *D. kappleri*, *D. hybridus*, and *D. septemcinctus* are wider with a shorter snout and relatively small braincase (negative values). A regression of the first principal component on the logarithm of the centroid size (Fig. 4B) clearly shows that the five species show different size ranges. The biggest crania are long and display longer and wider snout; whereas the smallest crania are short and wide posteriorly and characterized by a short snout. *D. pilosus* clearly remains an outlier once the size effect is removed (S5), while the other species appear less differentiated in the cranium morphospace. The specific differentiation was checked by performing a discriminant analysis and using a classification phase. The classification methods recovered 100% correct classification of specimens.

We also performed the same analyses this time including juvenile specimens (S6) but excluding *D. pilosus* since it represents a clear outlier in the morphospace. All juvenile specimens of *D. novemcintus* tend to congregate in the negative values of the PC1 and then appear more similar in shape to *D. septemcinctus* and *D. hybridus* than the adults. All juveniles of *D. novemcinctus* and *D. septemcinctus* are located in more negative values of PC1 and more positive values of PC2 relative to the adult individuals of their own species. Such a distribution in the morphospace defined by PC1-2 suggests similar ontogenetic trajectories for the two species.

Intraspecific variation of skull shape in nine-banded armadillos

In specimens for which sex was available (22 females and 32 males for the mandible; 19 females and 34 males for the cranium), a MANOVA shows that there is no sexual dimorphism present in the cranial data (Wilks' lambda=0.2429, F=1.514, p=0.182), so sex is unlikely to be responsible for the variation observed in the cranium of *D. novemcinctus*, while it might partly for the mandible (Wilks' lambda=0.2292, F=2.579, p=0.0110). A multivariate regression of the shape component on size was highly significant (mandible, Wilks' lambda=0.3468, F=3.454, p <0.001; cranium, Wilks' lambda=0.1447, F=8.446, p <0.001). When looking at the allometric shape vectors obtained with the centroid size (S2B and S3B), we found that size explains 14.14% and

14.32% of the variation in the whole mandibular and cranial data sets respectively. Shape data corrected for allometry are presented in S7 and S8.

A weak intraspecific differentiation (per country) is noticeable on the mandibular morphology (mandible, Wilks' lambda=0.0001404, F=1.523, p <0.001; Fig. 5A). The first principal component (9.87% of total shape variation) weakly discriminates specimens from Brazil, Bolivia, Paraguay, Uruguay (positive values) from other specimens (negative values). This axis separates mandibles characterized by robust and short horizontal ramus and long ascending ramus with a high coronoid, low condylar, and poorly individualized angular processes from mandibles with slender and elongated horizontal ramus and short ascending ramus with low coronoid, high condylar, and well individualized angular processes (Fig. 5A). In terms of shape variation, PC2 (4.745% of total shape variation) separates mandibles that show elongated anterior part of the horizontal ramus, short tooth row, high and distally oriented coronoid process from mandibles having reduced anterior part of the horizontal ramus, an elongated tooth row, and low coronoid process. We observed even less differentiation with shape data corrected for allometry (S7), which indicates that some specimens differ significantly in size. This is confirmed by a regression of the first principal component on the logarithm of the centroid size (Fig. 5B) that shows that the specimens from Brazil, Uruguay, Paraguay, Bolivia, Peru, Ecuador, Costa Rica, and Colombia are usually smaller.

A MANOVA was also used to explore if the cranial variation matches the geographical distributions of *D. novemcinctus* (Wilks' lambda=2.97×10^{-6}, F=2.157, p <0.001). When looking at the cranial morphological variation according to geographic origin (*i.e.*, countries) (Fig. 6), several trends can be observed. PC1, accounting for 22.7% variation, demonstrates a change in how domed the dorsal surface of the skull is and positively correlates with an increase in snout length, a decrease in braincase size, jugals more extended dorsoventrally, and shorter pterygoid processes (Fig. 6A). Specific clusters are recognizable on the first principal component with specimens from Brazil, Paraguay, Venezuela (USNM 406700 from Clarines area, North), Ecuador (BMNH-14-4-25-86 from Gualaquiza, South East), Colombia (AMNH 136252 from Villavicencio area, Centre), Peru, Bolivia, Paraguay, and Uruguay that congregate in the negative values whereas all other specimens lay in the positive values. PC2 is responsible for 8.6% of the variance, and describes variation in the size of the posterior part of the rostrum; it also displays variation in length of the posterior part of the palate with an anterior border of the palatine that is well behind the posterior end of the tooth row in positive values. This axis mainly separates specimens from USA, Mexico, Belize, Honduras, Guatemala, and Nicaragua (negative values) from other specimens (positive values). We observed less specific differentiation with shape data corrected for allometry (S8), which shows that the different geographical subgroups differ significantly in size. This is confirmed by a regression of the first principal component to the logarithm of the centroid size (Fig. 7).

A Linear Discriminant Analysis (LDA) of shape coordinates was performed in order to take into account the entire morphological variation (*i.e.*, 35 first PCs that represent 90.6% of the variance) and to maximize discrimination among specimens belonging to different countries. Only countries for which we had several specimens could be considered here. Three main regional groups were clearly recovered by the analysis (Fig. 8A): a Northern morphotype, a Southern morphotype, and a group circumscribed to the Guiana Shield (GS). The first group from North and Central America includes specimens from the US, Mexico, Guatemala, and Belize. The South American group gathers specimens from Brazil, Uruguay, Bolivia, Peru, Colombia, and Venezuela. Finally, specimens from French Guiana, Suriname, and Guyana congregate in a last distinctive group. Some specimens from Colombia, Venezuela, and Ecuador do not gather with any of those groups and sit in the middle of the graph defined by the first two discriminant axes; these specimens are however well discriminated on the third and fourth discriminant axes (Fig. 8B) and might constitute a fourth individualized regional group among *D. novemcinctus*, called hereafter the Central morphotype.

The discriminant model used to separate the regional groups was checked using a classification phase and then used on under-sampled countries (*i.e.*, when n=1) to assess their affiliation to one of the four abovementioned groups. This classification showed 95% correct classification of specimens (S9). Most regional misclassifications were with specimens coming from the limit of the distribution range of the groups. Two Brazilian specimens from Amapa are put together with the Guianan specimens (S9) and confirmed previous results from the PCA where these two specimens clearly depart from the rest of the Brazilian specimens (Fig. 6A). Three specimens from Venezuela (USNM 406700 from Clarines area, North), Ecuador (BMNH-14-4-25-86 from Gualaquiza, South East), and Colombia (AMNH 136252 from Villavicencio area, Centre) were *a posteriori* classified as close to the Southern morphotype. All these specimens were collected East of the Andes (Fig. 9) and grouped with Brazilian specimens in the PCA analyses. Concerning the countries for which only one specimen was available, the classification analyses gave congruent results with the grouping proposed by the principal component analysis: specimens from Paraguay and Peru were classified as being part of the Southern morphotype while specimens from Nicaragua, Honduras, and Costa Rica were classified as grouping with the Northern morphotype (S9). Using a reduced set of landmarks, the specimen from Panama was attributed to the Central morphotype. When performing these classification methods using the four groups as factors (*i.e.*, Northern, Central, Southern, and

Guianan morphotypes; see S10), instead of countries, we retrieved 100% correct classification of specimens.

We performed very similar analyses (PCA and LDA, see S11) using linear cranial measurements traditionally used in systematic studies. In all cases, these analyses failed to retrieve a clear-cut discrimination between the four groups defined above.

Discussion

Morphological variation of skull among* Dasypus *species

Skull ratios are commonly used to compare *Dasypus* species, especially the length of the palate to length of skull (PL/CNL) and length of rostrum to length of skull (RL adj./CNL) (Wetzel, 1985). Three subgenera are commonly recognized on this basis: *Cryptophractus* (including *D. pilosus*), *Hyperoambon* (including *D. kappleri*), and *Dasypus* (including all remaining species) (Wetzel & Mondolfi, 1979). Our results are largely consistent with findings from previous studies regarding existing differences between *Dasypus* species. Allometry substantially explains cranial differences, with the exception of *D. pilosus* that does not follow the main dasypodine allometric trend (Figs. 3 and 4). The hairy long-nosed armadillo clearly departs from the other four *Dasypus* species in being mainly characterized by a lengthening of the snout and mandible and a small development of the braincase and basicranium. All these characteristics were linked to their unique diet, which might predominantly include ants and termites (Castro et al., 2015). Considering these distinctive morphological features and a specific structure of its osteoderms, Castro et al. (2015) recently proposed to include *D. pilosus* in a different genus, i.e. *Cryptophractus*. However, recent molecular results (Gibb et al., 2016) did not support such a taxonomic reassessment and argued for the conservation of the hairy long-nosed armadillo in the genus *Dasypus*. *D. pilosus* thus likely represents a case of rapid acquisition (*i.e.*, 2.8 Ma as estimated by Gibb et al., 2016) of distinctive morphological traits in line with the shift to a divergent behaviour and ecology.

Both molecular and morphological data suggested that *D. kappleri* is broadly separated from the other *Dasypus* species (Wetzel & Mondolfi, 1979; Gibb et al., 2016). Mitogenomic data clearly identified *D. kappleri* as the sister group to all other *Dasypus* species from which it diverged more than 12 million years ago (Gibb et al., 2016) and suggested to place it in the distinct genus *Hyperoambon*, as originally proposed by Wetzel and Mondolfi (1979). We retrieved a significant morphological differentiation with all the specimens of *D. kappleri* congregating in the morphospace and being much larger than the other species. However, the cranial morphology of *D. kappleri* still remains very close to that of *D. novemcinctus* when compared to that of *D. septemcinctus*, *D. hybridus*, and *D. pilosus* (Fig. 4). Recently, Feijo and Cordeiro-Estrela (2016) proposed to recognize three species within *D. kappleri* based on morphological differences of the skull and carapace: *D. kappleri* distributed in the Guiana shield; *D. pastasae* occurring from the eastern Andes of Peru, Ecuador, Colombia, and Venezuela south of the Orinoco River into the western Brazilian Amazon; and finally *D. beniensis* that occurs in the lowlands of the Amazonian Brazil and Bolivia to the south of the Madre de Dios, Madeira, and lower Amazon rivers. We only had access to a limited number of specimens but did not retrieve such a clear geographical segregation in shape (S12A), while we observed a mild differentiation in size with the Guianan *D. kappleri* being usually bigger (S12B).

Wetzel and Mondolfi (1979:47) placed *D. septemcinctus*, *D. hybridus*, and *D. sabanicola* in the same subgenus together with *D. novemcinctus*. We observed that *D. hybridus* and *D. septemcinctus* group together in the morphospace, but are largely separated from *D.*

novemcinctus. These two species are usually distinguished by external features, *D. hybridus* showing shorter ears and a longer tail than *D. septemcinctus* (Hamlett, 1939; Wetzel & Mondolfi, 1979). Our morphometrical results showed that *D. hybridus* and *D. septemcinctus* display very similar cranial and mandibular morphologies; they also display several cranial characteristics in common with juvenile specimens of *D. novemcinctus*. Such morphological similarities echo recent molecular findings (Gibb et al., 2016) that showed that mitogenomic sequences of *D. hybridus* are almost identical to those of an Argentinian *D. septemcinctus* (99.3% identity). The two species were considered as valid based on cranial and body measurements (Hamlett, 1939; Wetzel, 1985) despite the fact that they display many external resemblances and have very close geographical distribution. A recent study of their internal cranial sinuses also failed to provide diagnostic characters for the distinction of these two genera (Billet et al., unpublished data). Our samples were very limited for both *D. hybridus* (n=4) and *D. septemcinctus* (n=3), but additional samplings will undoubtly help to define the systematic status of the two species.

We did not have access to the two most recently recognized *Dasypus* species: the Yunga's lesser long-nosed armadillo *D. mazzai* (Yepes, 1933), and the northern long-nosed armadillo *D. sabanicola* (Mondolfi, 1967). The validity of the former was and is still hotly debated (Wetzel & Mondolfi, 1979; Vizcaíno, 1995; Gardner, 2008; Feijo & Cordeiro-Estrela, 2014), while the specific status of the latter also remains controversial (Wetzel & Mondolfi, 1979; Wetzel, 1985). Cranial morphometric data might provide insightful arguments to discuss the systematic status of the two species.

Morphological systematics and skull shape variation in **Dasypus**

Relative skull shape has previously been examined for systematics purposes in the genus *Dasypus* but never with a focus on patterns of intraspecific variation. Hamlett (1939) casted doubt on the possibility to identify different subgroups within *D. novemcinctus*, while early workers had already recognized several, either at a specific or at a subspecific level. Peters (1864) described *Dasypus fenestratus* from Costa Rica based on the position of the small and numerous major palatine foramina, some of which are connected to the incisive foramina through a groove, between (not in front of) the anterior teeth, its medially shorter palatine bones, the position of the palatine suture posterior to the end of the tooth row, the position of the lacrimal foramen closer to the orbital rim, as well as one character on the extent of the pelvic shield of the carapace. Gray (1873) tentatively recognized as many as seven species of nine-banded armadillos in South and Central Americas, among which five of them were new: *Tatusia* (=*Dasypus*) *granadiana*, *T. leptorhynchus*, *T. brevirostris*, *T. leptocephala*, and *T. boliviensis*. He also followed Peters (1864) and recognized *T. mexicana* (a variety of *D. novemcinctus* in Peters 1864), but decided to ignore *T. fenestratus*. Both Peters (1864) and Gray (1873) used a very small number of specimens and Gray (1873) distinguished all these species based mainly on the morphology of the lacrimal bones and minute morphological variation of the head scutes. Allen (1911) later considered *D. fenestratus* and *D. mexicanus* as synonym taxa of subspecific level (*D. novemcinctus fenestratus* Peters). He also described *D. novemcinctus hoplites* from Grenada, a subspecies that he considered to be distinctly characterized by a shorter tooth row due to the absence of the last tooth locus.

From the inspection of a series of specimens from Panama, Costa Rica, and Yucatan, Allen (1911) also distinguished a Central American morphotype. Compared to Brazilian specimens, Allen's Central American armadillo is characterized by short palatine bones that do not reach the level of the most posterior teeth, an obvious inflation of the maxillary region located in front of the lacrimal bone, as well as a lateral margin of the skull that is largely convex at the level of the second or third tooth in ventral view. Based on size differences, Hagmann (1908) described the subspecies *D. n. mexianae*, which he thought was restricted to a small area close to the mouth of the Amazon River. Lönnberg (1913) defined *D. n. aequatorialis* from Ecuador, which McBee and Baker (1982) later proposed to consider as a probable synonym to *T. granadiana* Gray 1873. His comparisons were based on morphological characteristics of the carapace, *D. n. aequatorialis* showing differences of the occipital portion of the frontal shield as well as different proportions of the scales of the shoulder and pelvic shields. Later on, Russel (1953) proposed to recognize two subspecies in Mexico: *D. n. davisi* in north-western part of Mexico and *D. n. mexicanus* present in most of the country. Even if it is close morphologically to *D. n. mexicanus*, *D. n. davisi* is much smaller in size and displays a few distinctive features such as small maxillary teeth, a narrow mandible with an angular process posteriorly projected, and differences in suture closure patterns and shape with for instance the parietal-frontal sutures that lies well behind the posterior process of the zygomatic arch (Russell, 1953). Most of these early descriptions, be them at a specific and subspecific level, were based on subtle morphological differences and no proper quantification of the skull variation was undertaken up to now.

Our statistical analysis of the skull shape demonstrated that *D. novemcinctus* exhibits a significant level of intraspecific variation, with several clearly identified groups within the nine-banded armadillo. While male nine-banded armadillos tend to be slightly larger than females (McBee & Baker, 1982), our multivariate analyses first suggest the absence of sexual dimorphism in the cranium and a slight sexual dimorphism in the mandible. We also show that allometry is likely to explain a substantial part of the observed morphological variation, including geographically. This echoes early findings by Wetzel and Mondolfi (1979) who already pointed out size gradients between different populations of *D. novemcinctus*. Our morphometric analysis successfully retrieved such a geographical differentiation, both in size and shape. Interestingly, our geometric morphometric analyses permitted to define four discrete phenotypic units. These units display very different cranial characters and occupy very distinct geographical distributions, which are in essence allopatric.

Specimens from Brazil, Uruguay, Paraguay, Bolivia, Peru, and from regions of Ecuador, Colombia, and Venezuela located east of the Andes make up most of one group and show a very stable pattern of variation (Fig. 9); they are on average smaller than the three remaining groups. Skulls of this Southern morphotype are clearly distinct by showing smaller and flatter skulls with short frontal sinuses, a narrow snout with short premaxillar bones, a narrow interorbital width, a long and slender jugal part of the zygomatic arch, longer pterygoid processes, and a basicranium aligned with the palate in lateral view (Fig. 6). We found no sign of morphological differentiation of specimens from the mouth of the Amazon River, as implied by the proposed recognition of the subspecies *D. n. mexianae* (Hagmann, 1908). The area covered by the specimens attributed to this morphological unit fully encompasses that of the Amazon basin and seemed to be delimitated by the Andes on the western side. As a matter of fact, the single Ecuadorian specimen coming from the eastern side of the Andes appeared to be distinct from most other Ecuadorian specimens, but morphologically close to Brazilian and Bolivian specimens. The same holds true for the Peruvian, Colombian, and Venezuelan specimens collected east of the Andes. The distribution of this group is reminiscent of that of the subspecies *D. novemcinctus novemcinctus* Linnaeus, except for the Guiana Shield area (Gardner, 2008). It also recalls a similar lineage molecularly identified (Arteaga et al., unpublished data) and the

Southern morphotype evidenced by the analysis of paranasal spaces (Billet et al., unpublished data). Unfortunately the type specimen of *D. novemcinctus*; which is supposedly housed in the Swedish Museum of Natural History in Stockholm (Lönnberg, 1913), could not be included in our analyses. The type locality of *Dasypus novemcinctus* Linnaeus is "America meridionali" and is generally thought to be from the eastern coast of Brazil (Allen, 1911).

The next differentiated group is represented by individuals originating from the Guiana shield region including French Guiana, Guyana, Suriname, and Amapa in Brazil (Fig. 9). All the specimens belonging to this Guianan morphotype display large dome-shaped skulls that share distinctive morphological features including long frontal sinuses, a wide snout with long premaxillar bones, a large interorbital width, large lacrimal bones, a short and massive jugal part of the zygomatic arch, an anterior border of the palatine located well behind the posterior end of the tooth row, shorter pterygoid processes, and a basicranium situated above the palatal plane (Fig. 6). Studies of paranasal sinuses agree with the distinctness of this group and show that the dome-shaped frontal region of Guianan nine-banded armadillos is occupied by a characteristically inflated pair of frontal sinuses that extend posteriorly to the fronto-parietal suture (Billet al., unpublished data). No subspecies has ever been recognized or proposed in this part of South America, and such a clear-cut morphological divergence of Guianan specimens of *D. novemcinctus* is here proposed for the first time. These morphometric findings corroborate recent molecular studies, which showed that specimens from French Guiana are very distant from the US populations (Huchon et al., 1999) and represent a distinct branch in the dasypodine mitogenomic tree (Gibb et al., 2016; Arteaga et al., submitted).

The distribution of the third recognized morphological group is more limited. It is distributed from the western Andes of Ecuador, Colombia, Panama, and Venezuela to Costa Rica

(Fig. 9). This Central morphotype is characterized by high and short skulls having moderately developed frontal sinuses, long premaxillar bones, a narrow interorbital width (larger than Southern specimens but narrower than Guianan specimens), a massive anterior part of the zygomatic arch that is much larger than the posterior part, a short and high jugal part of the zygomatic arch that is largely convex ventrally, an anterior border of the palatine located well behind the posterior end of the tooth row, shorter pterygoid processes, and a basicranium well above the palatal plan (Fig. 6). This distribution roughly corresponds to the combined ranges of two previously described subspecies: *D. n. fenestratus* (Peters, 1864) and *D. n. aequatorialis* (Lönnberg, 1913). These close morphological resemblances suggest that these subspecies might be synonym taxa. However, we could not fully test this hypothesis since we had only access to one specimen from West of the Andes in Peru, Ecuador and southern Bolivia. Studies on the paranasal spaces (Billet et al., unpublished data) failed to recognize such a group, and instead gathered some specimens from these regions with specimens from North and Central America, while others (from the western parts of Colombia, Venezuela and from Panama) were judged impossible to be confidently referred to a given frontal sinus morphotype. In contrast, molecular studies recovered a lineage similar to the group recognized here distributing from the Northern Andes and Central America but expanding to western Mexico (Arteaga et al., unpublished data).

The last distinct morphotype occurs from Nicaragua to the Southern part of the US (Fig. 9). The range of this Northern morphotype spans the proposed distribution areas of the subspecies *D. n. mexicanus* and *D. n davisi*, as well as the northernmost part of the distribution range of *D. n. fenestratus*. All the skulls from this area display moderately developed frontal sinuses convergent toward the midline, long premaxillar bones, a narrow interorbital width (larger than Southern specimens but narrower than Guianan specimens), a long and slender jugal part of the zygomatic arch that is largely convex ventrally, an anterior border of the palatine located at the level of the posterior end of the tooth row, shorter pterygoid processes, and a basicranium slightly above the palatal plan (Fig. 6). Contrary to Russel (1953), we did not find major morphological cranial differences between north-western and eastern Mexican populations. Our results thus cast doubts on the validity of the subspecies *D. n. davisi*. The morphological homogeneity in this group is also at odds with the presence of two mitochondrial lineages in Mexico (Arteaga et al., 2012, submitted) but is coherent with the presence of nuclear gene flow between them (Arteaga et al., 2011). Within this Northern group, the invasive US armadillo population derived from two geographical sources: one from Mexico and one from south-central Florida where captive animals were presumably released (Loughry & Mcdonough, 2013). For a long time, the exact origin of the Floridian introduced population remained uncertain. All the US specimens used in our analyses were proved to belong to the same Northern morphotype. Echoing the results obtained on six microsatellite loci described by Loughry et al. (2009), we interpret our findings as indicative of a close relationship between the two US populations. The recognition of this Northern unit with individuals ranging from Central to Northern America is also in agreement with their distinctive pattern of paranasal sinuses (Billet et al., unpublished data).

The newly recognized subgroups within *D. novemcinctus* prompt questions about the role of ecological factors likely to have influenced their morphological differentiation. Morphological variation in skull morphology as a result of ecological factors has been studied in a number of species over recent years (*e.g.*, Caumul and Polly, 2005; Wroe and Milne, 2007; Hautier et al., 2012). Factors such as temperature, diet and competition may cause phenotypic variation and are likely to explain some morphological differences between the identified groups. These ecological factors vary in relation to geography, and differences in geographical distribution can drive selection for different phenotypes, which may eventually lead to distinctive populations or even new species. Since the four *D. novemcinctus* subgroups are not sympatric in most of their respective natural range, we can hypothesize that environment and/or genetic drift, but not competition, may be responsible for some of the observed intraspecific variation. The Northern Andes constitute a clear geographical barrier, which limited contacts between Northern/Central and Southern populations, and thus has likely played a major role in shaping the morphological differentiation of the long-nosed armadillos. This biogeographical barrier seems to have played a significant role in xenarthrans since it also marks the separation between the two living species of tamanduas with *Tamandua mexicana* in the north and *T. tetradactyla* in the south (Superina, Miranda & Abba, 2010), also within naked-tailed armadillos with *Cabassous centralis* in the north and *C. unicinctus* in the south (Abba & Superina, 2010).

The geographical distribution of the divergent populations of *D. novemcinctus* recalls the pattern of morphological differentiation recently proposed for the greater long-nosed armadillo (*D. kappleri*), especially for the Guianan specimens (Feijo & Cordeiro-Estrela, 2016). However, in the nine-banded armadillo, we did not find a clear morphological differentiation within the Amazonian basin as defined on the opposite banks of the Madeira-Madre de Dios rivers (Feijo & Cordeiro-Estrela, 2016), which separate *D. pastasae* from *D. beniensis*. Given the extent of morphological variation reported within *D. kappleri*, Feijo and Cordeiro-Estrela (2016) interpreted their findings as indicative of the fact that this species complex diverged earlier than other *Dasypus* species, which would allow them to accumulate more differences. Such a hypothesis seems difficult to conceive in view of the substantial morphological variation observed among different populations of *D. novemcinctus*, which have diverged more recently

(3.7 Ma, Gibb et al., 2016). Feijo and Cordeiro-Estrela (2016) also proposed that such cumulative differences may result from strong environmental selective pressures. The newly discovered morphological diversity within *D. kappleri* and *D. novemcinctus* is likely to represent parallel cases of allopatric differentiation in response to diverging environmental pressures. In both cases, only the future collecting of large-scale genomic nuclear data will allow testing these taxonomic proposals based on morphological data.

Conclusions

Intraspecific variations can be the result of adaptation to varying local environmental conditions. We showed that morphometrical comparisons enable detection of previously overlooked morphotypes and yield new insights into factors likely to explain differences between populations inhabiting different areas. Our study of the intraspecific variation of the skull in *D. novemcinctus* evidences clear links to the geographic distribution and allows a revision of past taxonomic delimitations. Based on the cranial differences observed, we consider that *D. novemcinctus* should be regarded either as a polytypic species (with three to four subspecies) or as a complex of several species. In particular, a new unit of nine-banded armadillos from the Guiana Shield could be detected, which is in agreement with most recent investigations of molecular data and internal anatomy (Arteaga et al., unpublished data; Billet et al., unpublished data). The discovery of divergent populations within *D. novemcinctus* has implications for conservation of the species. In some areas, human activities have led to habitat degradation and fragmentation (Zimbres et al., 2013) or even to habitat loss. These divergent populations may be under threat and may require conservation measures, or at least a close re-examination of their conservation status. If we were to consider them as separate management unit and not as a single species with a large distribution, the threat of endangerment to *D. novemcinctus* would need re-evaluation since it is currently classified globally as 'Least Concern' by the IUCN (Loughry, McDonough & Abba, 2014). In addition, our results demonstrate that specimens of *D. novemcinctus* should be chosen with caution when making anatomical comparisons or performing cladistic analyses (*e.g.*, Castro et al., 2015); their geographical distribution should be at least specified in all cases. This morphological investigation needs to be extended to the other parts of the body, the carapace in particular. The cranial differences detected among the defined groups might be linked to previously detected differences in the number and shape of scutes on the head shield (*e.g*., Lönnberg, 1913). Geometric morphometric data holds out the possibility of studying effectively covariation patterns between osteological parts and features of the carapace. Given the quality of the cingulate fossil record, using geometric morphometric methods seems equally conceivable on extinct forms and might also provide fruitful ways to interpret past morphological diversity.

Acknowledgements

We are grateful to Christiane Denys, Violaine Nicolas, and Géraldine Véron, (Muséum National d'Histoire Naturelle, Paris), Roberto Portela Miguez, Louise Tomsett and Laura Balcells (British Museum of Natural History, London), Eileen Westwig (American Museum of Natural History, New-York), Burton Lim (Royal Ontario Museum, Toronto), Nicole Edmison and Chris Helgen (National Museum of Natural History, Washington), Jake Esselstyn (Louisiana State University, Bâton-Rouge), Manuel Ruedi (*Muséum d'Histoire naturelle*, Geneva), Claudia Regina da Silva (*Instituto de Pesquisas Científicas e Tecnológicas do Estado do Amapá*, Macapá), Steven van der Mije (Naturalis Biodiversity Center, Leiden), François Cazeflis and Suzanne Jiquel (Institut des Sciences de l’Evolution, Montpellier), Lucile Dudoignon (KWATA association), Dominique Charles (CNRS), Maria-Clara Arteaga, Maria Nazareth da Silva (*Instituto de Pesquisas Científicas e Tecnológicas do Estado do Amapá*) for access to comparative material. We thank Clara Belfiore for her help in the data acquisition. R. Lebrun (Institut des Sciences de l’Evolution, Montpellier), Farah Ahmed (British Museum of Natural History, London), Miguel García-Sanz and Florent Goussard (Platform AST-RX MNHN) generously provided help and advice on the acquisition of CT scans. Some of the experiments were performed using the µ-CT facilities of the Montpellier Rio Imaging (MRI) platform and of the LabEx CeMEB. This is contribution ISEM 2017-XXX of the Institut des Sciences de l’Evolution.

Funding

This work has benefited from an "Investissements d’Avenir' grant managed by Agence Nationale de la Recherche, France (CEBA, ref. ANR-10-LABX-25-01). This research received support from the Synthesys Project (http://synthesys3.myspecies.info/), which is financed by the European Community Research Infrastructure Action under the FP7.

Grant Disclosures

The following grant information was disclosed by the authors:

Agence Nationale de la Recherche: contract ANR-10-LABX-25-01.

Competing Interests

The authors declare no competing interests.

Author Contributions

- Lionel Hautier conceived and designed the experiments, contributed materials, performed the experiments, analysed the data, wrote the paper.
- Guillaume Billet conceived and designed the experiments, contributed materials.
- Benoit de Thoisy contributed materials.
- Frédéric Delsuc conceived and designed the experiments, contributed materials.
- All authors read, discussed, corrected, and approved the final version of the paper.

Data Deposition

The following information was supplied regarding the deposition of related data:

Dryad, http://dx.doi.org/xxxxx.

References

Abba AM., Superina M. 2010. The 2009/2010 armadillo red list assessment. *Edentata* 11:135–184.

Allen G. 1911. Mammals of the west indies. *Bulletin of the useum of Comparative Zoology* 54:175–263.

Arteaga MC., McCormack JE., Eguiarte LE., Medellín RA. 2011. Genetic admixture in multidimensional environmental space: asymmetrical niche similarity promotes gene flow in armadillos (*Dasypus novemcinctus*). *Evolution* 65:2470–2480.

Arteaga MC., Piñero D., Eguiarte LE., Gasca J., Medellín R. 2012. Genetic structure and diversity of the nine-banded armadillo in Mexico. *Journal of Mammalogy* 93:547–559.

Asher RJ., Lehmann T. 2008. Dental eruption in afrotherian mammals. *BMC biology* 6:14. DOI: 10.1186/1741-7007-6-14.

Bookstein F. 1991. *Morphometric tools for landmark data. Geometry and biology*. Cambridge: Cambridge University Press.

Carlini A a., Castro MC., Madden RH., Scillato-Yané GJ. 2013. A new species of Dasypodidae (Xenarthra: Cingulata) from the late Miocene of northwestern South America: implications in the Dasypodini phylogeny and diversity. *Historical Biology*:37–41. DOI: 10.1080/08912963.2013.840832.

Carlini A., Vizcaíno S., Scillato-Yané G. 1997. Armored xenarthrans: a unique taxonomic and ecologic assemblage. In: Kay R, Madden R, Cifelli R, Flynn J. eds. *Vertebrate paleontology in the Neotropics. The Miocene Fauna of La Venta, Colombia*. Washington/London: Smithsonian Institution Press, 213–226.

Castro MC. 2015. Sistemática y evolución de los armadillos Dasypodini (Xenarthra, Cingulata, Dasypodidae). *Revista del Museo de La Plata* 15:1–50.

Castro MC., Avilla LS., Freitas ML., Carlini AA. 2013a. The armadillo Propraopus sulcatus (Mammalia: Xenarthra) from the late Quaternary of northern Brazil and a revised synonymy with Propraopus grandis. *Quaternary International* 317:80–87. DOI: 10.1016/j.quaint.2013.04.032.

Castro MC., Carlini A a., Sánchez R., Sánchez-Villagra MR. 2014. A new Dasypodini armadillo (Xenarthra: Cingulata) from San Gregorio Formation, Pliocene of Venezuela: Affinities and biogeographic interpretations. *Naturwissenschaften* 101:77–86. DOI: 10.1007/s00114-013-1131-5.

Castro MC., Ciancio MR., Pacheco V., Salas-Gismondi RM., Bostelmann JE., Carlini AA. 2015. Reassessment of the hairy long-nosed armadillo "*Dasypus*"*pilosus* (Xenarthra, Dasypodidae) and revalidation of the genus *Cryptophractus* Fitzinger, 1856. *Zootaxa* 3947:30–48. DOI: 10.11646/zootaxa.3947.1.2.

Castro MC., Ribeiro AM., Ferigolo J., Langer MC. 2013b. Redescription of *Dasypus punctatus* Lund, 1840 and considerations on the genus *Propraopus* Ameghino, 1881. *Journal of Vertebrate Paleontology* 33:434–447. DOI: 10.1080/02724634.2013.729961.

Caumul R., Polly P. 2005. Phylogenetic and environmental components of morphological variation: skull, mandible, and molar shape in marmots (*Marmota*, Rodentia). *Evolution* 59:2460–2472.

Ciancio MR., Castro MC., Asher RJ. 2012. Evolutionary implications of dental eruption in *Dasypus* (Xenarthra). *Journal of Mammalian Evolution* 19:1–8. DOI: 10.1007/s10914-011-9177-7.

Delsuc F., Superina M., Tilak M., Douzery EJP., Hassanin A. 2012. Molecular Phylogenetics and Evolution Molecular phylogenetics unveils the ancient evolutionary origins of the enigmatic fairy armadillos. *Molecular Phylogenetics and Evolution* 62:673–680. DOI: 10.1016/j.ympev.2011.11.008.

Dryden I., Mardia K. 1998. *Statistical shape analysis*. Chichester: John Wiley & Sons.

Feijo A., Cordeiro-Estrela P. 2014. The correct name of the endemic *Dasypus* (Cingulata: Dasypodidae) from northwestern Argentina. *Zootaxa* 3887:88–94. DOI: 10.11646/zootaxa.3887.1.6.

Feijo A., Cordeiro-Estrela P. 2016. Taxonomic revision of the *Dasypus kappleri* complex, with revalidations of *Dasypus pastasae* (Thomas, 1901) and *Dasypus beniensis* Lönnberg, 1942 (Cingulata, Dasypodidae). *Zootaxa* 4170:271–297. DOI: 10.11646/zootaxa.4170.2.3.

Gardner AF. 2008. *Mammals of South America Volume 1 Marsupials, Xenarthrans, Shrews, and Bats*. Chicago and London: The University of Chicago Press.

Gaudin TJ., Wible JR. 2006. The Phylogeny of Living and Extinct Armadillos (Mammalia, Xenarthra, Cingulata): A Craniodental Analysis. In: Carrano M, Gaudin TJ, Blob R, Wible JR eds. *Amniote Paleobiology: Perspectives on the Evolution of Mammals, Birds and Reptiles*. Chicago: The University of Chicago Press, 153–198.

Gibb GC., Condamine FL., Kuch M., Enk J., Moraes-Barros N., Superina M., Poinar HN., Delsuc F. 2016. Shotgun mitogenomics provides a reference phylogenetic framework and timescale for living xenarthrans. *Molecular Biology and Evolution* 33:621–642. DOI: 10.1093/molbev/msv250.

Gray J. 1873. *Handlist of the edentate, thick-skinned, and ruminant mammals of the British Museum*. London: British Museum of Natural History.

Hagmann G. 1908. Die Landsäugetiere der insel Mexiana. Als Beispiel der Einwirkung der isolation auf die umbildung der arten. *Arch. Rass.-Gesell.-Biol. München* 5:1–32.

Hamlett G. 1939. Identity of *Dasypus septemcinctus* Linnaeus with notes on some related species. *Journal of Mammalogy* 20:328–336.

Hammer Ø., Harper D., Ryan P. 2001. PAST: paleontological statistics software package for education and data analysis. *Paeontologica Electronica* 4:9.

Hautier L., Billet G., Eastwood B., Lane J. 2014. Patterns of Morphological Variation of Extant Sloth Skulls and their Implication for Future Conservation Efforts. *Anatomical Record* 297:979–1008. DOI: 10.1002/ar.22916.

Hautier L., Lebrun R., Cox PG. 2012. Patterns of covariation in the masticatory apparatus of hystricognathous rodents: implications for evolution and diversification. *Journal of morphology* 273:1319–37. DOI: 10.1002/jmor.20061.

Hensel R. 1872. *Beiträge zur Kenntnis der Säugethiere Süd-Brasiliens*. Berlin: lis den Abhandlungen der Königl. Akademie der Wissenschaften.

Huchon D., Delsuc F., Catzeflis F., Douzery EJP. 1999. Armadillos exhibit less genetic polymorphism in North America than in South America: nuclear and mitochondrial data confirm founder effect in *Dasypus novemcinctus* (Xenarthra). *Molecular Ecology* 8:1743–1748.

Lebrun R. 2008. Evolution and development of the strepsirrhine primate skull. University Montpellier II and University of Zürich.

Lebrun R. 2014. ISE-MeshTools, a 3D interactive fossil reconstruction freeware. In: *12th Annual Meeting of EAVP*. Torino,.

Lebrun R., Ponce de León M., Tafforeau P., Zollikofer C. 2010. Deep evolutionary roots of strepsirrhine primate labyrinthine morphology. *Journal of Anatomy* 216:368–380.

Linnaeus C. 1758. *Systema Naturae, Ed; 10. L.* Uppsala: Salvii.

Lönnberg E. 1913. Mammals from Ecuador and related forms. *Arkiv för Zoologi* 8:1–36.

Loughry WJ., Mcdonough CM. 1998. Comparisons between nine-banded armadillo (*Dasypus novemcinctus*) populations in brazil and the united States. *Revista de biología tropical* 46:1173–1183.

Loughry WJ., Mcdonough CM. 2013. *The nine-banded armadillo: a natural history*. Norman: University of Oklahoma Press.

Loughry J., McDonough C., Abba A. 2014. *Dasypus novemcinctus*. *The IUCN Red List of Threatened Species* 2014:e.T6290A47440785.

Loughry WJ., Truman RW., McDonough CM., Tilak M-K., Garnier S., Delsuc F. 2009. Is leprosy spreading among nine-banded armadillos in the southeastern United States? *Journal of Wildlife Diseases* 45:144–152. DOI: 10.7589/0090-3558-45.1.144.

McBee K., Baker RJ. 1982. *Dasypus novemcinctus*. *Mammalian Species* 162:1–9.

Mondolfi E. 1967. Descripción de un nuevo armadillo del género *Dasypus* de Venezuela (Mammalia-Edentata). *Memorias de la Sociedad de Ciencias Naturales La Salle* 78:149–167.

Peters W. 1864. Über neue Arten de Saugethier-gattungen *Geomys*, *Haplodon* und *Dasypus*. *Monatsbericht der Königlich- Preussischen Akademie der Wissenschaften zu Berlin* 1865:177–181.

Rohlf F. 1999. Shape statistics: Procrustes superimpositions and tangent spaces. *Journal of Classification* 16:197–223.

Russell R. 1953. Description of a new armadillo (Dasypus novemcinctus) from mexico with remarks on geographic variation of the species. *Proceedings of the Biological Society of*

Washington 66:21–26.

Smith L., Doughty R. 1984. The amazing armadillo: geography of a folk critter. In: Austin: University of Texas Press, 134.

Specht M. 2007. Spherical surface parameterization and its application to geometric morphometric analysis of the braincase. University of Zürich Irchel.

Specht M., Lebrun R., Zollikofer C. 2007. Visualizing shape transformation between chimpanzee and human braincases. *The Visual Computer* 23:743–751.

Superina M., Miranda FR., Abba AM. 2010. The 2010 anteater red list assessment. *Edentata* 11:96–114.

Taulman JF., Robbins LW. 2014. Range expansion and distributional limits of the nine-banded armadillo in the United States: an update of Taulman & Robbins (1996). *Journal of Biogeography* 41:1626–1630.

Vizcaíno SF. 1995. Identificacion especifica de las "mulitas', genero Dasypus L. (Mammalia; Dasypodidae); del noroeste argentino. Descripcion de una nueva especie. *Mastozoologia Neotropical* 2:5–13.

Wetzel R. 1985. Taxonomy and distribution of armadillos. In: *The Evolution and Ecology of Armadillos, Sloths, and Vermilinguas*. Washington DC: Smithsonian Institution Press, 23–46.

Wetzel R., Mondolfi E. 1979. The subgenera and species of long-nosed armadillos, genus *Dasypus*. In: Eisenberg J ed. *Vertebrate Ecology in the Northern Neotropic*. Washington DC: Smithsonian Institution Press, 43–63.

Wilson D., Reeder D. 2005. *Mammal species of the world: a taxonomic and geographic reference. 3rd ed.* Baltimore: Johns Hopkins University Press.

Wroe S., Milne N. 2007. Convergence and remarkably consistent constraint in the evolution of carnivore skull shape. *Evolution* 61:1251–1260.

Yepes J. 1933. Una especie nueva de “mulita” (Dasypodinae) para el norte argentino. *Physis* 11:225–232.

Zimbres B., Furtado MM., Jácomo, Anah T. A. Silveira L., Sollmann R., Tôrres NM., Machado RB., Marinho-Filho J. 2013. The impact of habitat fragmentation on the ecology of xenarthrans (Mammalia) in the Brazilian Cerrado. *Lanscape Ecology* 28:259–269.

Table legends

Table 1. Definitions of the landmarks used on the mandible.

Table 2. Definitions of the landmarks used on the cranium. Landmarks indicated with a star were not used in the intraspecific comparisons.

Figure Legends

Figure 1. Landmarks digitized on the mandible and the skull. Dorsal (A), lateral (B), and ventral views of the cranium; medial (C) and lateral (D) views of the mandible.

Figure 2. Illustration of the skull linear measurements. In blue, traditional measurements used in Wetzel (1985). *Abbreviations*: LTC, length between the anterior tip of the nasal and the posteriormost point of the supraoccipital; LR, rostral length; IOB, interorbital breadth; ILFB, inter lacrimal foramina breadth; BB, distance between the left and right intersections between the frontal, parietal, and squamosal sutures; NB, nasal breadth; NL, nasal length; LCB, length between the anterior tip of the premaxillar and the condyles; TL, length of the tooth row; PB, palate breadth; BZP, distance between the infraorbital and the maxillary foramina; MB, inter-meatus breadth; OCB, breadth between the lateral border of the occipital condyle.

Figure 3. (**A**) Principal component analysis (PC1 *vs* PC2) and associate patterns of morphological transformation for the mandible of five *Dasypus* species. (**B**) Regression of the first principal component on the logarithm of the centroid size (R^2=0.23; p<0.001). *Symbols*: blue squares, *D. kappleri*; black crosses, *D. novemcinctus*; green triangles, *D. hybridus*; green diamonds, *D. septemcinctus*; red circles, *D. pilosus*.

Figure 4. (**A**) Principal component analysis (PC1 *vs* PC2) and associate patterns of morphological transformation for crania of five *Dasypus* species. (**B**) Regression of the first principal component on the logarithm of the centroid size (R^2=0.55; p<0.001). *Symbols*: blue

squares, *D. kappleri*; black crosses, *D. novemcinctus*; green triangles, *D. hybridus*; green diamonds, *D. septemcinctus*; red circles, *D. pilosus*.

Figure 5. (**A**) Principal component analysis (PC1 *vs* PC2) and associate patterns of morphological transformation for mandibles of *Dasypus novemcinctus*. (**B**) Regression of the first principal component on the logarithm of the centroid size (R^2=0,035; p=0.03). *Symbols*: green diamonds, Bolivia; green triangle, Brazil (solid green triangles are for specimens from Amapa); green circles, Paraguay; green crosses, Peru; green squares, Uruguay; green bars, Venezuela; blue diamonds, Belize; blue "plus", Guatemala; blue bars, Honduras; Blue squares, Mexico; blue crosses, Nicaragua; blue triangles, USA; blue circles, Costa Rica; black triangles, Colombia; black crosses, Ecuador; black stars, Panama; orange squares, French Guiana; orange crosses, Guyana; orange circles, Suriname.

Figure 6. Principal component analysis (**A**, PC1 *vs* PC2; **B**, PC3 *vs* PC4) and associate patterns of morphological transformation for crania of *Dasypus novemcinctus*. *Symbols*: green diamonds, Bolivia; green triangle, Brazil (solid green triangles are for specimens from Amapa); green circles, Paraguay; green crosses, Peru; green squares, Uruguay; green bars, Venezuela; blue diamonds, Belize; blue "plus", Guatemala; blue bars, Honduras; Blue squares, Mexico; blue crosses, Nicaragua; blue triangles, USA; blue circles, Costa Rica; black triangles, Colombia; black crosses, Ecuador; orange squares, French Guiana; orange crosses, Guyana; orange circles, Suriname.

Figure 7. Regression of the first cranial principal component (*Dasypus novemcinctus*) on the

logarithm of the centroid size ($R^2=0.15$; $p<0.001$). *Symbols*: green diamonds, Bolivia; green triangle, Brazil (solid green triangles are for specimens from Amapa); green circles, Paraguay; green crosses, Peru; green squares, Uruguay; green bars, Venezuela; blue diamonds, Belize; blue “plus”, Guatemala; blue bars, Honduras; Blue squares, Mexico; blue crosses, Nicaragua; blue triangles, USA; blue circles, Costa Rica; black triangles, Colombia; black crosses, Ecuador; orange squares, French Guiana; orange crosses, Guyana; orange circles, Suriname.

Figure 8. Linear Discriminant Analysis (LDA) performed on cranial shape coordinates of *Dasypus novemcinctus*. *Symbols*: green diamonds, Bolivia; green triangle, Brazil (solid green triangles are for specimens from Amapa); green circles, Paraguay; green crosses, Peru; green squares, Uruguay; green bars, Venezuela; blue diamonds, Belize; blue “plus”, Guatemala; blue bars, Honduras; Blue squares, Mexico; blue crosses, Nicaragua; blue triangles, USA; black triangles, Colombia; black circles, Costa Rica; black crosses, Ecuador; orange squares, French Guiana; orange crosses, Guyana; orange circles, Suriname.

Figure 9. Summary map showing the geographical distribution of nine-banded armadillo specimens investigated in this study and their attribution to one of the four main morphotypes defined in this study: black, Central group; blue, Northern group; green, Southern group; orange, Guianan group. Specimens lacking precise geographical information (other than country of origin) are indicated with a square.

Supplemental Information

S1. List of measured specimens (used for linear measurements and/or geometric morphometric analyses). *Abbreviations:* MNHN, *Muséum national d'Histoire naturelle* in Paris (collections *Zoologie et Anatomie comparée, Mammifères et Oiseaux*); BMNH, Natural History Museum in London; NBC, Naturalis Biodiversity Center in Leiden; ROM, Royal Ontario Museum in Toronto; LSU, Louisiana State University in Bâton-Rouge; AMNH, American Museum of Natural History in New York; USNM, National Museum of Natural History in Washington; IEPA, *Instituto de Pesquisas Científicas e Tecnológicas do Estado do Amapá* in Macapá; MHNG, *Muséum d'Histoire naturelle* in Geneva; KWATA, KWATA association; and PCDPC, Personal collection of Pierre Charles-Dominique.

S2. Regression of the common allometric shape vector (ASVc) on the logarithm of the centroid size for mandibles of five *Dasypus* species (A, $R^2=0.50$; $p<0.001$) and *D. novemcinctus* (B, $R^2=0.34$; $p<0.001$). Below, associate patterns of morphological transformation for mandibles with small (left) and large (right) centroid size. *Symbols*: same as in Figure 3 and 5.

S3. Regression of the common allometric shape vector (ASVc) on the logarithm of the centroid size for crania of five *Dasypus* species (A, $R^2=0.72$; $p<0.001$) and *D. novemcinctus* (B, $R^2=0.48$; $p<0.001$). Below, associate patterns of morphological transformation for crania with small (left) and large (right) centroid size. *Symbols*: same as in Figure 3 and 5.

S4. Principal component analyses with shape data corrected for allometry (PCres1 *vs* PCres 2) and associate patterns of morphological transformation for mandible of five *Dasypus* species. *Symbols*: blue squares, *D. kappleri*; black crosses, *D. novemcinctus*; green triangles, *D. hybridus*; green diamonds, *D. septemcinctus*; red circles, *D. pilosus*.

S5. Principal component analyses with shape data corrected for allometry (PCres1 *vs* PCres 2) and associate patterns of morphological transformation for crania of five *Dasypus* species. *Symbols*: blue squares, *D. kappleri*; black crosses, *D. novemcinctus*; green triangles, *D. hybridus*; green diamonds, *D. septemcinctus*; red circles, *D. pilosus*.

S6. (**A**) Principal component analysis (PC1 *vs* PC2) and associate patterns of morphological transformation for crania of five *Dasypus* species, including juveniles (indicated with smaller symbols) and excluding *D. pilosus*. (**B**) Regression of the first principal component on the logarithm of the centroid size (R^2=0,63; p<0.001). *Symbols*: blue squares, *D. kappleri*; black crosses, *D. novemcinctus*; green triangles, *D. hybridus*; green diamonds, *D. septemcinctus*.

S7. Principal component analyses with shape data corrected for allometry (PCres1 *vs* PCres 2) and associate patterns of morphological transformation for mandibles of *Dasypus specimens*. *Symbols*: green diamonds, Bolivia; green triangle, Brazil (solid green triangles are for specimens from Amapa); green circles, Paraguay; green crosses, Peru; green squares, Uruguay; green bars, Venezuela; blue diamonds, Belize; blue “plus”, Guatemala; blue bars, Honduras; Blue squares, Mexico; blue crosses, Nicaragua; blue triangles, USA; blue circles, Costa Rica; black triangles, Colombia; black crosses, Ecuador; black stars, Panama; orange squares, French Guiana; orange crosses, Guyana; orange circles, Suriname.

S8. Principal component analyses with shape data corrected for allometry (PCres1 *vs* PCres 2) and associate patterns of morphological transformation for crania of *Dasypus specimens*. *Symbols*: green diamonds, Bolivia; green triangle, Brazil (solid green triangles are for specimens from Amapa); green circles, Paraguay; green crosses, Peru; green squares, Uruguay; green bars, Venezuela; blue diamonds, Belize; blue "plus", Guatemala; blue bars, Honduras; Blue squares, Mexico; blue crosses, Nicaragua; blue triangles, USA; blue circles, Costa Rica; black triangles, Colombia; black crosses, Ecuador; orange squares, French Guiana; orange crosses, Guyana; orange circles, Suriname.

S9. Results of *a posteriori* classifications for the discriminant analysis performed on the cranial shape coordinates of *Dasypus novemcinctus* using countries as factors. Specimens with a star (*) were integrated into the analyses as ungrouped cases.

S10. Results of *a posteriori* classifications for the discriminant analysis performed on the cranial shape coordinates of *Dasypus novemcinctus* using the four subgroups (*i.e.*, Northern, Central, Southern, and Guianan morphotypes) as factors. Specimens with a star (*) were integrated into the analyses as ungrouped cases.

S11. (**A**) Principal component analysis (PC1 *vs* PC2) and associate patterns of morphological transformation for crania of *Dasypus kappleri*. (**B**) Regression of the first principal component on the logarithm of the centroid size ($R^2=0.40$; $p<0.001$). *Symbols*: green crosses, Peru; green bars, Venezuela; black triangles, Colombia; black crosses, Ecuador; orange squares, French

Guiana; orange crosses, Guyana; orange circles, Suriname.

Figure 1

Figure 1

Landmarks digitized on the mandible and the skull. Dorsal (A), lateral (B), and ventral views of the cranium; medial (C) and lateral (D) views of the mandible.

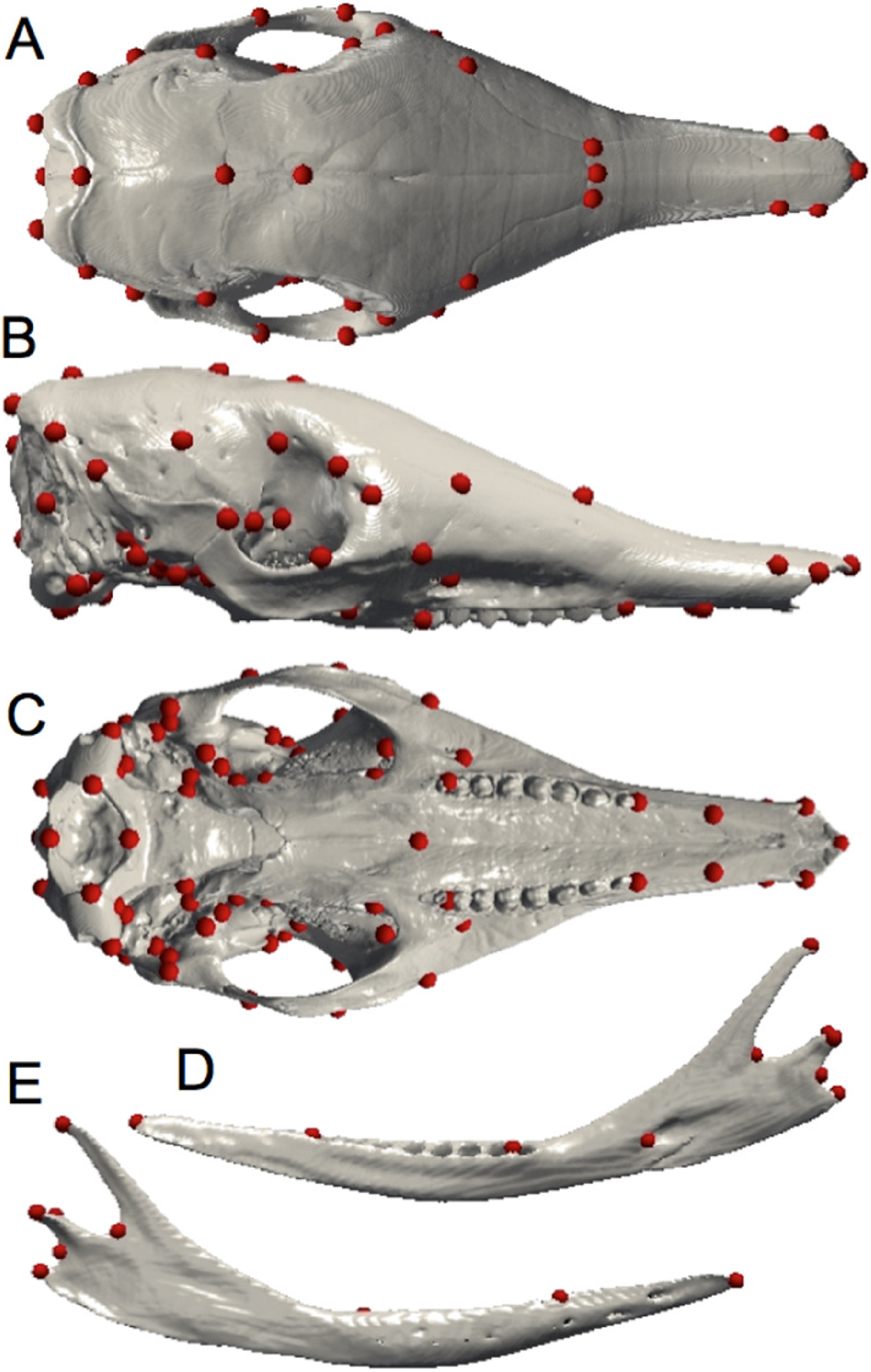
A
B
C
D
E

Figure 2

Figure 2

Illustration of the skull linear measurements. In blue, traditional measurements used in Wetzel (1985) . *Abbreviations*: LTC, length between the anterior tip of the nasal and the posteriormost point of the supraoccipital; LR, rostral length; IOB, interorbital breadth; ILFB, inter lacrimal foramina breadth; BB, distance between the left and right intersections between the frontal, parietal, and squamosal sutures; NB, nasal breadth; NL, nasal length; LCB, length between the anterior tip of the premaxillar and the condyles; TL, length of the tooth row; PB, palate breadth; BZP, distance between the infraorbital and the maxillary foramina; MB, inter-meatus breadth; OCB, breadth between the lateral border of the occipital condyle.

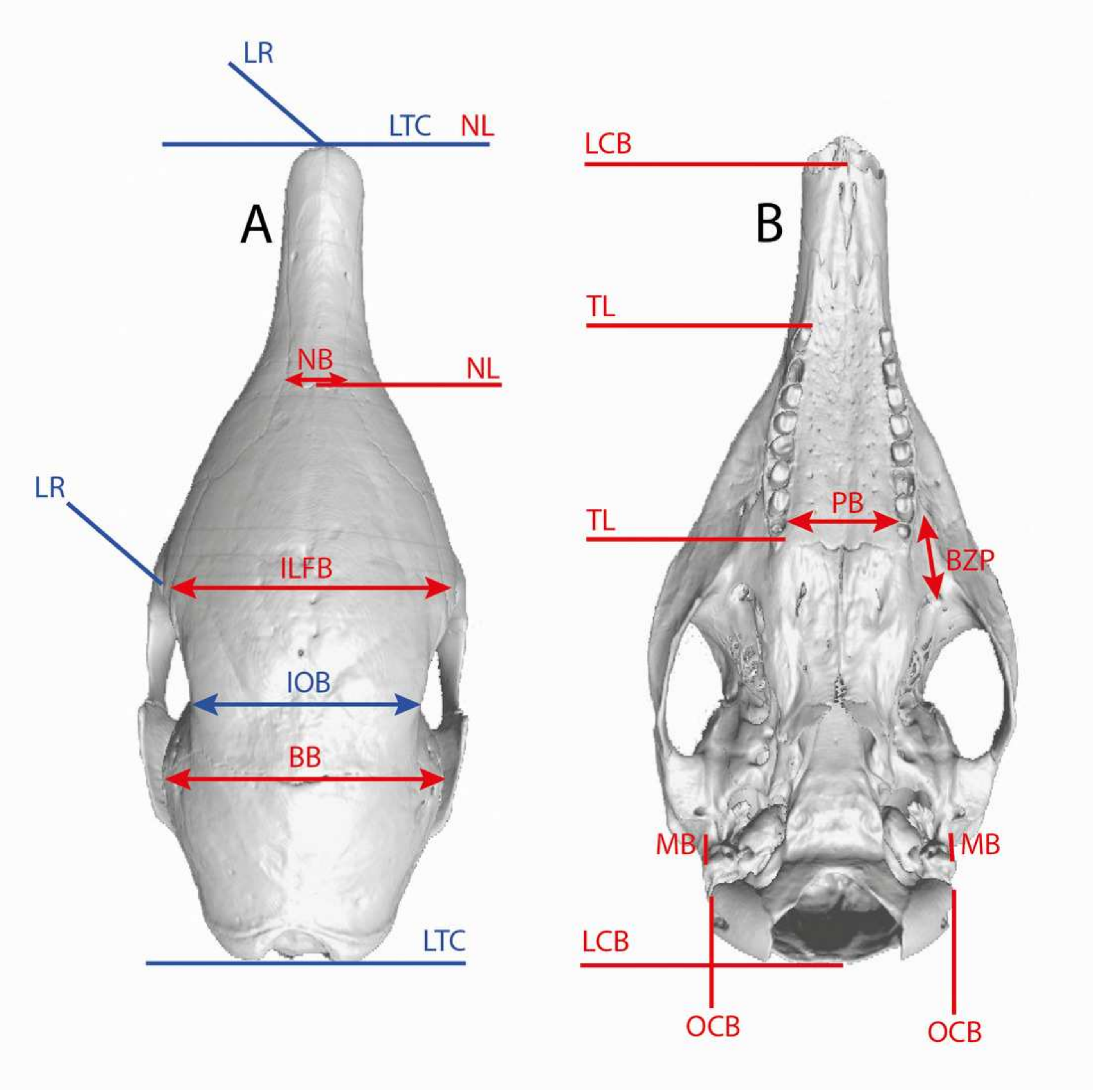
LR
LTC
NL
A
NB
NL
LR
ILFB
IOB
BB
LTC
LCB
B
TL
TL
PB
BZP
MB
MB
LCB
OCB
OCB

Figure 3

Figure 3

(**A**) Principal component analysis (PC1 *vs* PC2) and associate patterns of morphological transformation for the mandible of five *Dasypus* species. (**B**) Regression of the first principal component on the logarithm of the centroid size ($R^2=0.23$; $p<0.001$). *Symbols*: blue squares, *D. kappleri*; black crosses, *D. novemcinctus*; green triangles, *D. hybridus*; green diamonds, *D. septemcinctus*; red circles, *D. pilosus*.

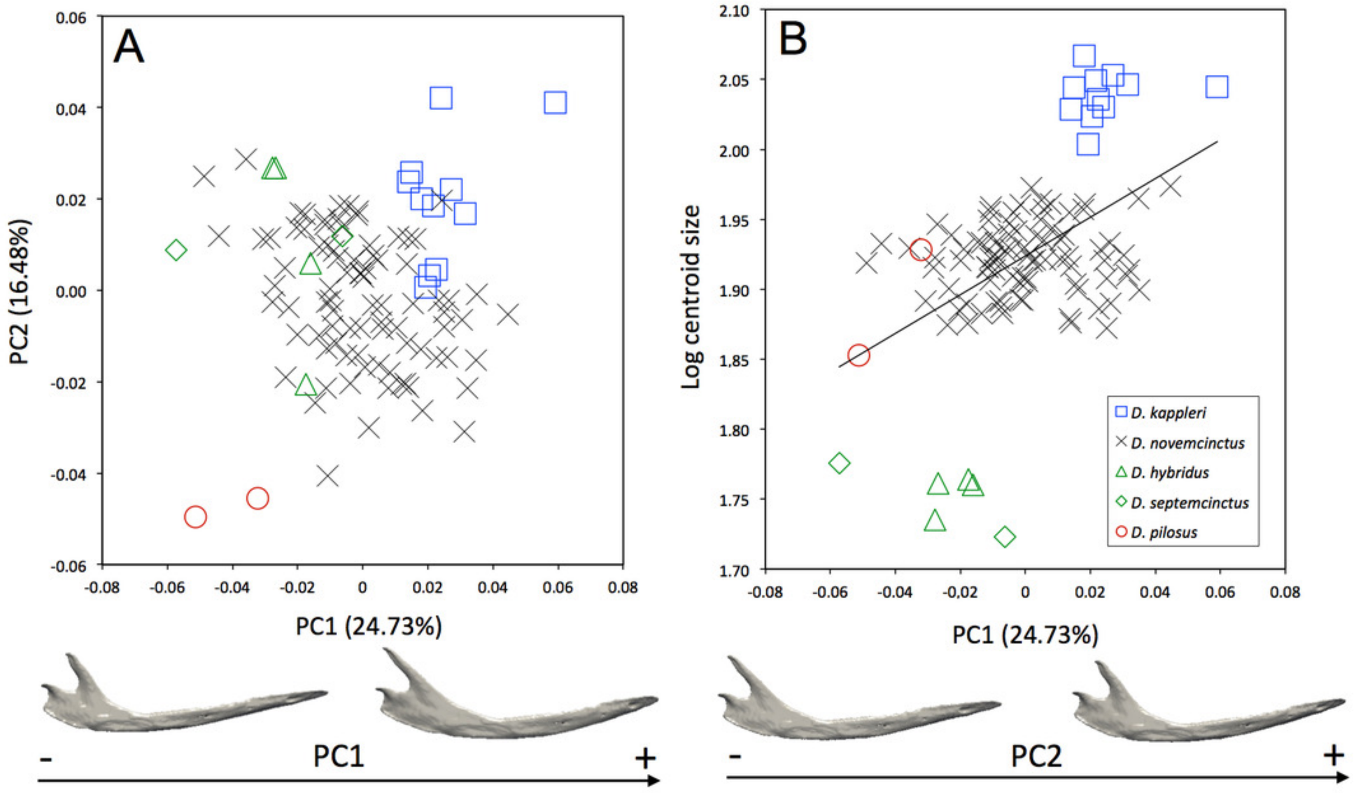

Figure 4

Figure 4

(**A**) Principal component analysis (PC1 *vs* PC2) and associate patterns of morphological transformation for crania of five *Dasypus* species. (**B**) Regression of the first principal component on the logarithm of the centroid size ($R^2=0.55$; $p<0.001$). *Symbols*: blue squares, *D. kappleri*; black crosses, *D. novemcinctus*; green triangles, *D. hybridus*; green diamonds, *D. septemcinctus*; red circles, *D. pilosus*.

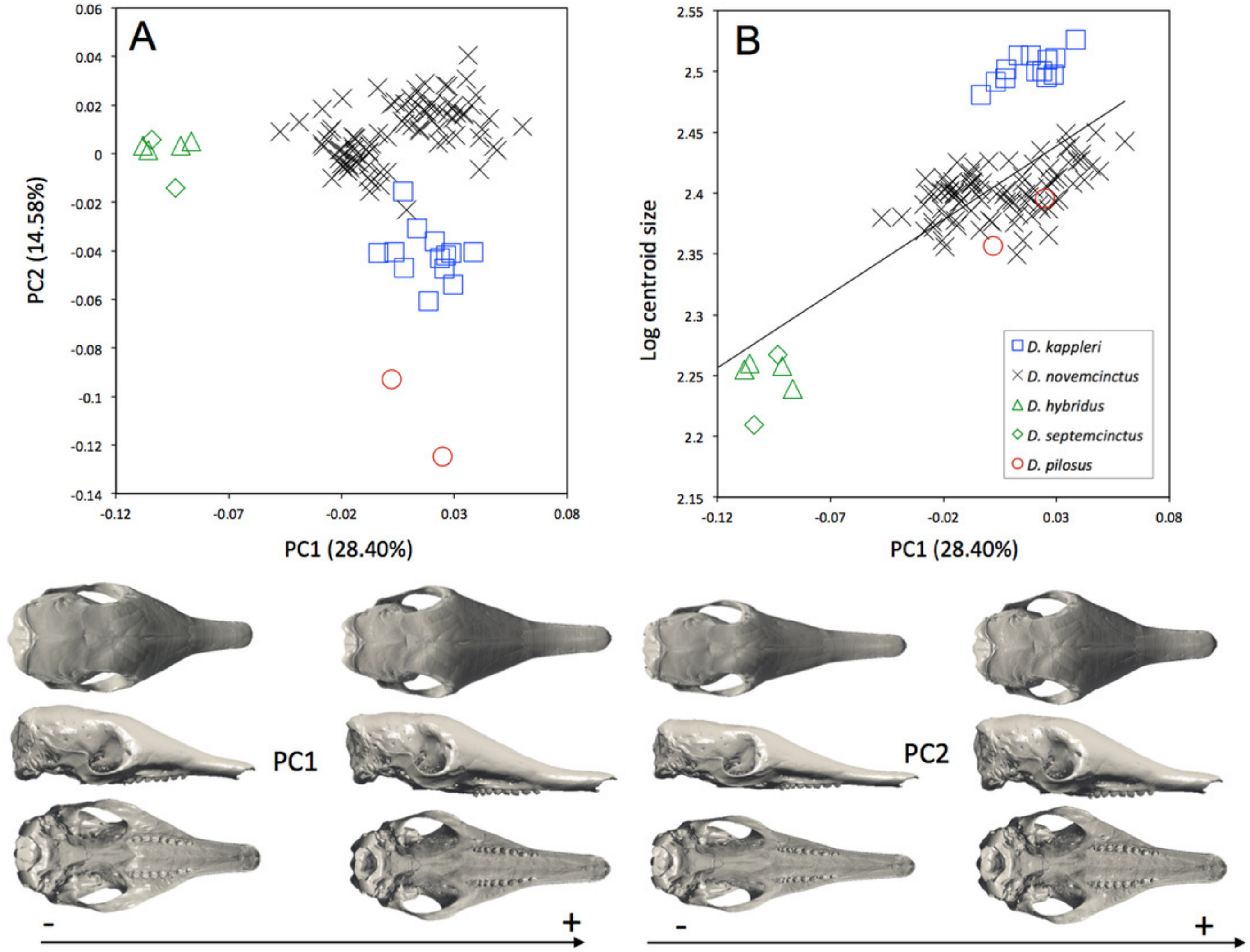

Figure 5

Figure 5

(**A**) Principal component analysis (PC1 *vs* PC2) and associate patterns of morphological transformation for mandibles of *Dasypus novemcinctus*. (**B**) Regression of the first principal component on the logarithm of the centroid size (R^2=0,035; p=0.03). *Symbols*: green diamonds, Bolivia; green triangle, Brazil (solid green triangles are for specimens from Amapa); green circles, Paraguay; green crosses, Peru; green squares, Uruguay; green bars, Venezuela; blue diamonds, Belize; blue “plus”, Guatemala; blue bars, Honduras; Blue squares, Mexico; blue crosses, Nicaragua; blue triangles, USA; blue circles, Costa Rica; black triangles, Colombia; black crosses, Ecuador; black stars, Panama; orange squares, French Guiana; orange crosses, Guyana; orange circles, Suriname.

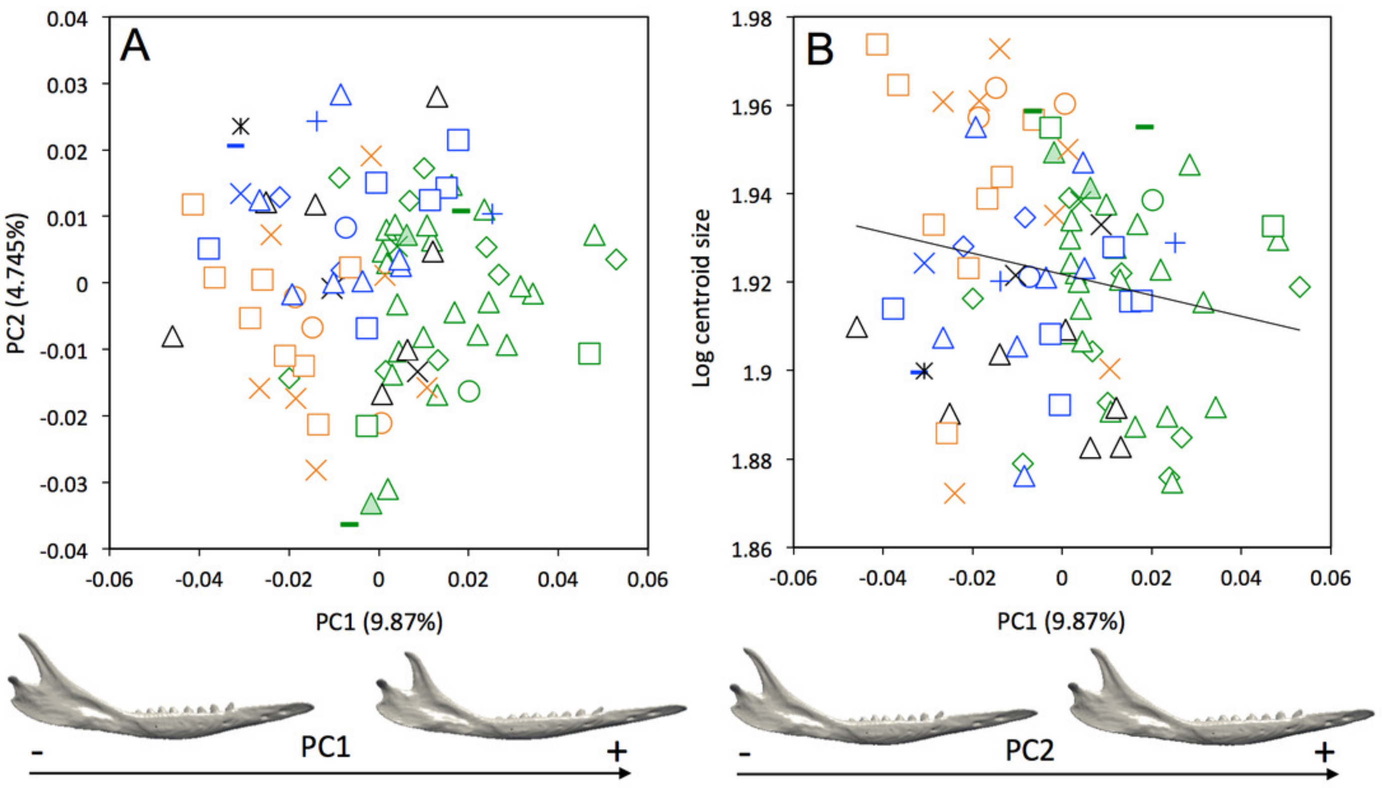

Figure 6

Figure 6

Principal component analysis (**A**, PC1 *vs* PC2; **B**, PC3 *vs* PC4) and associate patterns of morphological transformation for crania of *Dasypus novemcinctus*. *Symbols*: green diamonds, Bolivia; green triangle, Brazil (solid green triangles are for specimens from Amapa); green circles, Paraguay; green crosses, Peru; green squares, Uruguay; green bars, Venezuela; blue diamonds, Belize; blue “plus”, Guatemala; blue bars, Honduras; Blue squares, Mexico; blue crosses, Nicaragua; blue triangles, USA; blue circles, Costa Rica; black triangles, Colombia; black crosses, Ecuador; orange squares, French Guiana; orange crosses, Guyana; orange circles, Suriname.

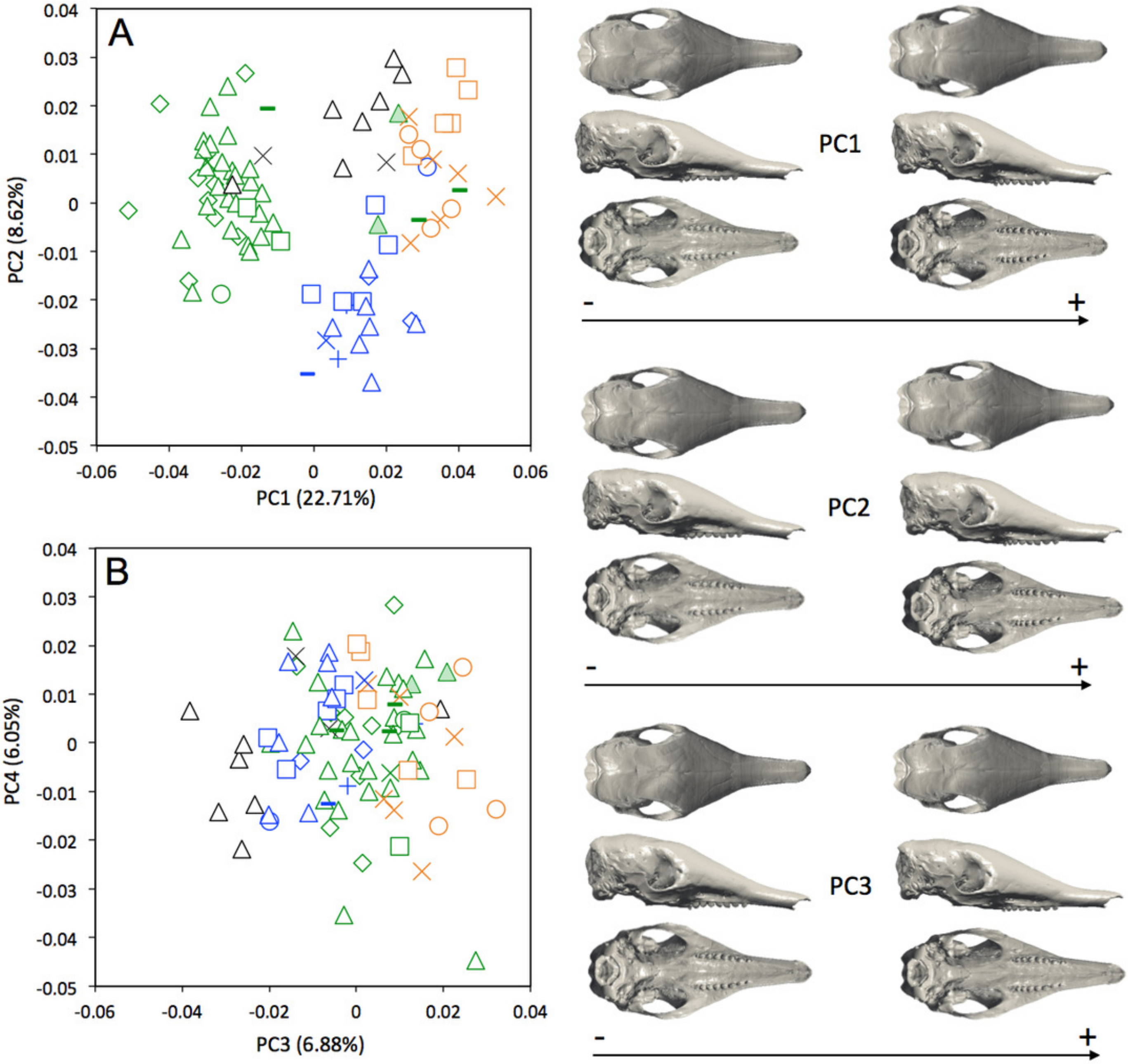
A
PC1 (22.71%)
PC2 (8.62%)
0.04
0.03
0.02
0.01
0
-0.01
-0.02
-0.03
-0.04
-0.05
-0.06
-0.04
-0.02
0
0.02
0.04
0.06
B
PC3 (6.88%)
PC4 (6.05%)
0.04
0.03
0.02
0.01
0
-0.01
-0.02
-0.03
-0.04
-0.05
-0.06
-0.04
-0.02
0
0.02
0.04
PC1
-
+
PC2
-
+
PC3
-
+

Figure 7

Figure 7

Regression of the first cranial principal component (*Dasypus novemcinctus*) on the logarithm of the centroid size (R^2=0.15; p<0.001). *Symbols*: green diamonds, Bolivia; green triangle, Brazil (solid green triangles are for specimens from Amapa); green circles, Paraguay; green crosses, Peru; green squares, Uruguay; green bars, Venezuela; blue diamonds, Belize; blue “plus”, Guatemala; blue bars, Honduras; Blue squares, Mexico; blue crosses, Nicaragua; blue triangles, USA; blue circles, Costa Rica; black triangles, Colombia; black crosses, Ecuador; orange squares, French Guiana; orange crosses, Guyana; orange circles, Suriname.

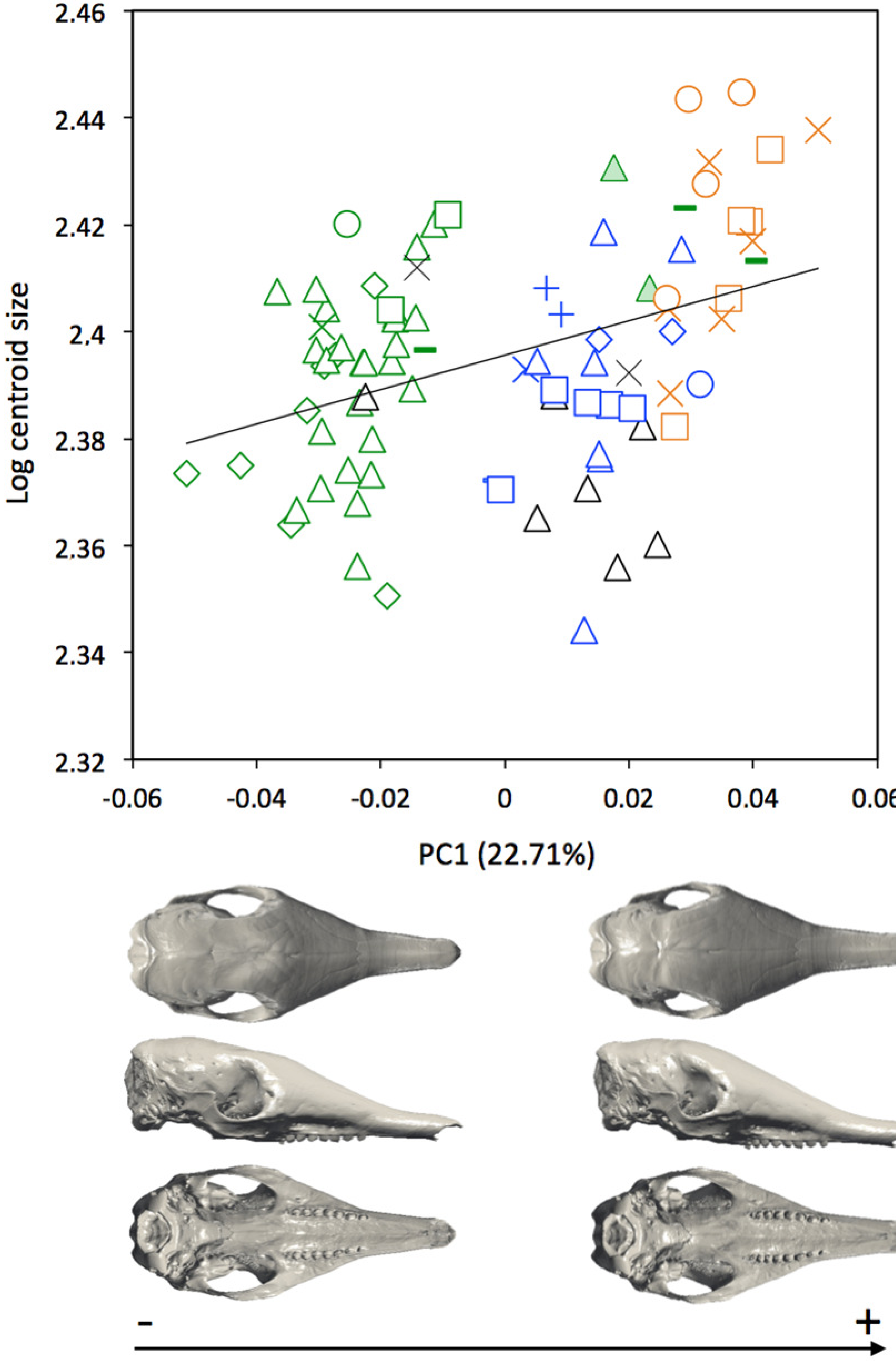
2.46
2.44
2.42
2.4
2.38
2.36
2.34
2.32
Log centroid size
-0.06
-0.04
-0.02
0
0.02
0.04
0.06
PC1 (22.71%)
-
+

Figure 8

Figure 8

Linear Discriminant Analysis (LDA) performed on cranial shape coordinates of *Dasypus novemcinctus*. *Symbols*: green diamonds, Bolivia; green triangle, Brazil (solid green triangles are for specimens from Amapa); green circles, Paraguay; green crosses, Peru; green squares, Uruguay; green bars, Venezuela; blue diamonds, Belize; blue “plus”, Guatemala; blue bars, Honduras; Blue squares, Mexico; blue crosses, Nicaragua; blue triangles, USA; black triangles, Colombia; black circles, Costa Rica; black crosses, Ecuador; orange squares, French Guiana; orange crosses, Guyana; orange circles, Suriname.

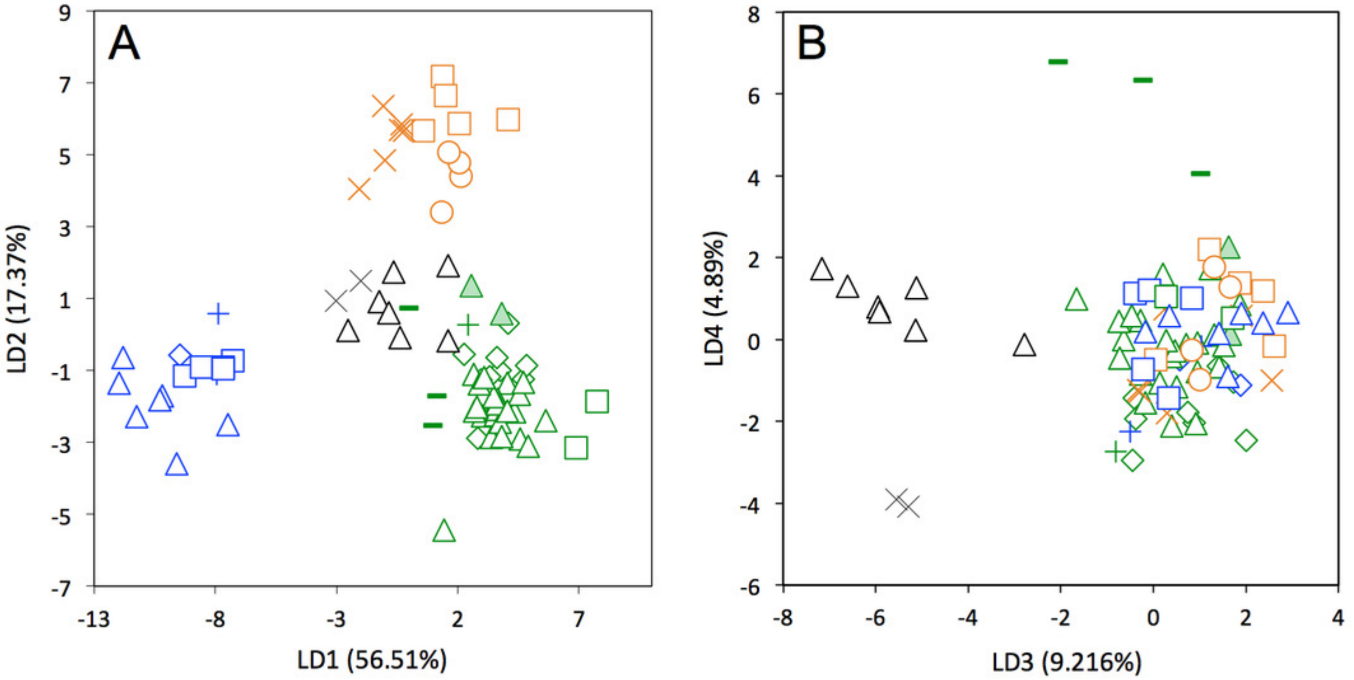

Figure 9

Figure 9

Summary map showing the geographical distribution of nine-banded armadillo specimens investigated in this study and their attribution to one of the four main morphotypes defined in this study: black, Central group; blue, Northern group; green, Southern group; orange, Guianan group. Specimens lacking precise geographical information (other than country of origin) are indicated with a square.

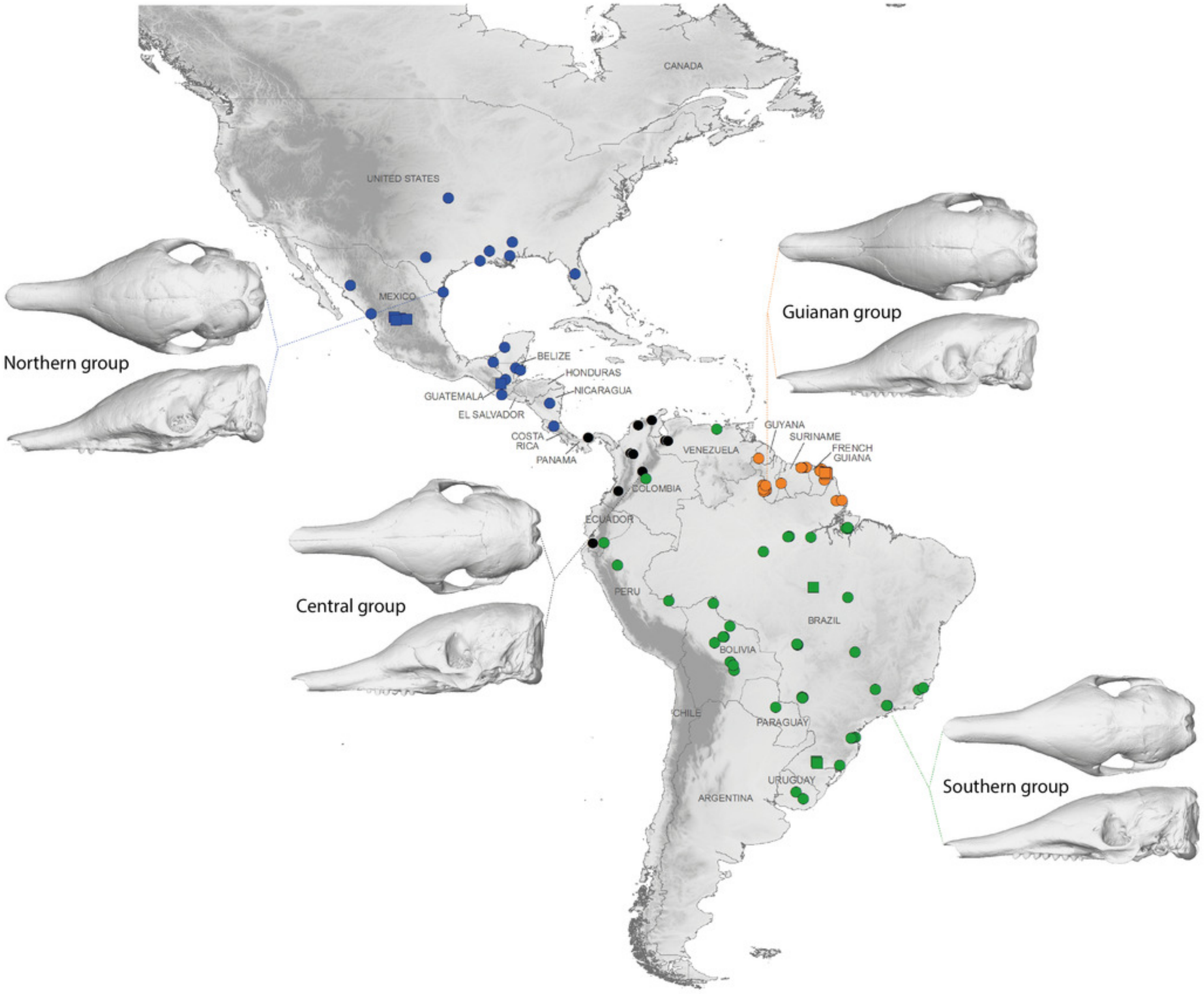

Table 1(on next page)

Table 1

Definitions of the landmarks used on the mandible

Numbers	Definition
1	Most anterior point of the mandible
2	Most anterior point of the alveolar margin of the tooth row
3	Most posterior point of the seventh tooth
4	Tip of the coronoid process
5	Point at the maximum of concavity between the coronoid and the condyloid processes
6	Most lateral point of the articular surface of the condyle
7	Most medial point of the articular surface of the condyle
8	Point at the maximum of concavity between the condyloid and the angular
9	Tip of the angular process
10	Mandibular foramen

Table 2(on next page)

Table 2

Definitions of the landmarks used on the cranium. Landmarks indicated with a star were not used in the intraspecific comparisons.

Numbers	Definition
1	Most anterodorsal point of the nasal suture
2	Intersection between inter-nasal and inter-frontal sutures
3	Intersection between inter-parietal and inter-frontal sutures
4	Intersection between inter-parietal and supra-occipal
5	Most distal point of the supra-occipal
6 and 7	Intersection between frontal, maxillar, and nasal sutures
8 and 9	Most dorsomedial point of the orbit (i.e. minimal interobital length)
10 and 11	Most posterolateral point of the supra-occipital
12 and 28	Most anterolateral point of the premaxillar/nasal suture
13 and 29	Intersection between premaxillar, maxillar, and nasal sutures
14 and 30	Interection between the lacrimal, maxillar, and frontal sutures
15 and 31	Anteroventral margin of the lacrimal foramen
16 and 32	Anteroventral margin of the upper ethmoid foramen
17 and 33	Most anterior point of the squamosal, frontal, and alisphenoid sutures
18 and 34	Most dorsal point of the maxillary foramen
19 and 35	Most dorsal point of the infraorbital foramen
20 and 36	Most anteroventral point of the sphenopalatine fissure
21 and 37	Most dorsal point of the jugal/maxillar suture
22 and 38	Most dorsal point of the jugal/squamosal suture
23 and 39	Most posterior point of the postglenoid process
24 and 40	Most posterodorsal point of the zygomatic part of the squamosal
25 and 41	Intersection between the frontal, squamosal, and parietal sutures
26 and 42	Most dorsal point of sulcus for external acoustic meatus on squamosal
27 and 43	Intersection between the parietal, squamosal, and supraoccipital sutures
44 and 60	Most posterior point of the premaxillar/maxillar suture in ventral view
45 and 61	Most anterior point of the alveolar margin of the tooth row
46 and 62	Most posterior point of the alveolus of the seventh dental locus
47 and 63	Intersection between the lacrimal/maxillar suture and the zygomasseteric crest in ventral view
48	Intersection between maxillar and palatine sutures
49 and 64	Most posterolateral point of the pterygoid wings
50 and 65	Transverse canal foramen
51 and 66	Most anterodorsal point of the *foramen ovale*
52 and 67	Most ventral of the alisphenoid/squamosal suture
53 and 68	Most lateral point between the basioccipital/basisphenoid sutures
54 and 69	Most posterolateral point of the jugular foramen
55 and 70	Most posterolateral point of the hypoglossal foramen
56 and 71	Most anterolateral point of the occipital condyle
57 and 72	Intersection between the basioccipital, the occipital condyle, and the *foramen magnum*
58	Most antero-ventral point of the *foramen magnum*
59	Most postero-dorsal point of the *foramen magnum*
73 and 74	Intersection between the supraoccipital, exoccipital, and petrosal sutures
75 and 76	Most posterior point of the postglenoid foramen
77 and 78	Caudal palatine foramen
79* and 80*	Point of maximum concavity on the maxillar/frontal suture in dorsal view
81 and 82	Intersection between the lacrimal/frontal suture and the orbit
83	Most posterior point of the frontal sinuses in the midline
84	Ventral tip of the tentorial process